# International Ocean Discovery Program

# Expedition 367 Preliminary Report

## South China Sea Rifted Margin

## Testing hypotheses for lithosphere thinning during continental breakup: drilling at the South China Sea rifted margin

**7 February–9 April 2017**

Zhen Sun, Joann Stock, Adam Klaus, and the Expedition 367 Scientists

IODP
INTERNATIONAL OCEAN
DISCOVERY PROGRAM

## Publisher's notes

## Disclaimer

## Copyright

## Citation

Sun, Z., Stock, J., Klaus, A., and the Expedition 367 Scientists, 2018. *Expedition 367 Preliminary Report: South China Sea Rifted Margin.* International Ocean Discovery Program. https://doi.org/10.14379/iodp.pr.367.2018

# Expedition 367 participants

## Expedition 367 scientists

**Zhen Sun**
**Co-Chief Scientist**
  CAS Key Laboratory of Ocean and Marginal Sea Geology
  South China Sea Institute of Oceanology
  China
  **zhensun@scsio.ac.cn**

**Joann M. Stock**
**Co-Chief Scientist**
  Division of Geological and Planetary Sciences
  California Institute of Technology
  USA
  **jstock@gps.caltech.edu**

**Adam Klaus**
**Expedition Project Manager/Staff Scientist**
  International Ocean Discovery Program
  Texas A&M University
  USA
  **aklaus@iodp.tamu.edu**

**Jacopo Boaga**
**Petrophysics (Physical Properties) Specialist**
  Dipartimento di Gioscienze
  Università degli Studi di Padova
  Italy
  **jacopo.boaga@unipd.it**

**Anne Briais**
**Petrophysics (Physical Properties) Specialist**
  Observatoire Midi-Pyrenes
  Centre National de la Recherche Scientifique
  France
  **anne.briais@cnrs.fr**

**Yifeng Chen**
**Inorganic Geochemist**
  Guangzhou Institute of Geochemistry
  Chinese Academy of Sciences
  China
  **yfchen@gig.ac.cn**

**Michael J. Dorais**
**Inorganic Geochemist**
  Department of Geological Sciences
  Brigham Young University
  USA
  **dorais@byu.edu**

**Akira Furusawa**
**Paleontologist (foraminifers)**
  Department of Geoscience
  Shimane University
  Japan
  **zerozaki.1130@gmail.com**

**Jessica L. Hinojosa**
**Sedimentologist**
  Division of Geological and Planetary Sciences
  California Institute of Technology
  USA
  **jess.l.hinojosa@gmail.com**

**Tobias W. Höfig**
**Petrologist**
  International Ocean Discovery Program
  Texas A&M University
  USA
  **hoefig@iodp.tamu.edu**

**Kan-Hsi Hsiung**
**Sedimentologist**
  Japan Agency for Marine-Earth Science and Technology
  Japan
  **hsiung@jamstec.go.jp**

**Baoqi Huang**
**Paleontologist (foraminifers)**
  Department of Geology
  Peking University
  China
  **bqhuang@pku.edu.cn**

**Xiao-Long Huang**
**Petrologist**
  Guangzhou Institute of Geochemistry
  Chinese Academy of Sciences
  China
  **xlhuang@gig.ac.cn**

**Benjamin G. Johnson**
**Sedimentologist**
  Geology and Geography
  West Virginia University
  USA
  **bgjohnson@mix.wvu.edu**

**Chao Lei**
**Petrophysics (Physical Properties) Specialist**
  Department of Marine Science
  College of Marine Science and Technology
  China University of Geosciences
  China
  **clei@cug.edu.cn**

**Li Li**
**Organic Geochemist**
  State Key Laboratory of Marine Geology
  Tongji University
  China
  **lilitju@tongji.edu.cn**

**Zhifei Liu**
**Sedimentologist**
State Key Laboratory of Marine Geology
Tongji University
China
**lzhifei@tongji.edu.cn**

**Antonio Luna**
**Petrologist**
Department of Geology
University of South Florida, Tampa
USA
**aluna2@mail.usf.edu**

**Claudia Lupi**
**Paleontologist (nannofossils)**
Department of Earth and Environmental Sciences
Università degli Studi di Pavia
Italy
**claudia.lupi@unipv.it**

**Anders J. McCarthy**
**Petrologist**
Institute of Earth Sciences
University of Lausanne
Switzerland
**anders.mccarthy@unil.ch**

**Michael Nirrengarten**
**Structural Geologist**
Institut de Physique du Globe de Strasbourg
France
**m.nirrengarten@unistra.fr**

**Caroline Robinson**
**Sedimentologist**
School of Earth Sciences
Ohio State University
USA
**robin5cm@dukes.jmu.edu**

**Isabel Sauermilch**
**Petrophysics (Physical Properties) Specialist**
Institute of Marine and Antarctic Studies (IMAS)
University of Tasmania
Australia
**isabel.sauermilch@utas.edu.au**

**Steven M. Skinner**
**Paleomagnetist**
Department of Geology
California State University, Sacramento
USA
**steven.skinner@csus.edu**

**Xiang Su**
**Paleontologist (nannofossils)**
CAS Key Laboratory of Ocean and Marginal Sea Geology
South China Sea Institute of Oceanology, Chinese Academy of
    Sciences
China
**suxiang@scsio.ac.cn**

**Rong Xiang**
**Paleontologist (foraminifers)**
CAS Key Laboratory of Ocean and Marginal Sea Geology
South China Sea Institute of Oceanology, Chinese Academy of
    Sciences
China
**rxiang@scsio.ac.cn**

**Rajeev Yadav**
**Petrophysics (Physical Properties) Specialist**
Department of Marine Geophysics
National Centre for Antarctic and Ocean Research (NCAOR)
India
**ryadav@ncaor.gov.in**

**Liang Yi**
**Paleomagnetist**
State Key Laboratory of Marine Geology
Tongji University
China
**yi.liang82@gmail.com**

**Cuimei Zhang**
**Structural Geologist**
CAS Key Laboratory of Ocean and Marginal Sea Geology
South China Sea Institute of Oceanology, Chinese Academy of
    Sciences
China
**cmzhang@scsio.ac.cn**

**Jinchang Zhang**
**Petrophysics (Physical Properties) Specialist**
CAS Key Laboratory of Ocean and Marginal Sea Geology
South China Sea Institute of Oceanology, Chinese Academy of
    Sciences
China
**jzhang@scsio.ac.cn**

**Yang Zhang**
**Paleomagnetist**
Department of Earth and Atmospheric Sciences
Purdue University
USA
**zhan2214@purdue.edu**

**Ning Zhao**
**Sedimentologist**
Department of Geology and Geophysics
Woods Hole Oceanographic Institution
USA
**ningzhao2009@hotmail.com**

**Lifeng Zhong**
**Petrologist**
School of Marine Sciences
Sun Yat-Sen University
China
**zhonglf@scsio.ac.cn**

## Observer

**Chih-Chieh Su**
**Sedimentologist/Observer**
   Institute of Oceanography
   National Taiwan University
   Taiwan
   **donccsu@ntu.edu.tw**

## Education and outreach

**Alessia Cicconi**
**Education/Outreach Officer**
   Liceo Classico "F. Stabili - E. Trebbiani" Ascoli Piceno
   School of Science and Technology
   Geology Division
   University of Camerino
   Italy
   **alessia.cicconi@unicam.it**

**Jiansong Zhang**
**Education/Outreach Officer**
   China
   **13311669691@163.com**

## SIEM Offshore AS officials

**Terry Skinner**
**Master of the Drilling Vessel**

**Sam McLelland**
**Offshore Installation Manager**

## Technical support

**Robert Aduddell**
Engineer

**Alexis Armstrong**
X-Ray Laboratory

**Heather Barnes**
Assistant Laboratory Officer

**Chad Broyles**
Curatorial Specialist

**Michael Cannon**
Marine Computer Specialist

**Etienne Claassen**
Marine Instrumentation Specialist

**Ty Cobb**
Physical Properties Laboratory

**William Crawford**
Senior Imaging Specialist

**Benjamin Daniel**
Core Laboratory

**Roy Davis**
Laboratory Officer

**David Fackler**
Applications Developer

**Seth Frank**
Thin Section Laboratory

**Edwin Garrett**
Paleomagnetism Laboratory

**Rachael Gray**
Core Laboratory

**Jan Jurie Kotze**
Marine Instrumentation Specialist

**Zenon Mateo**
Underway Geophysics Laboratory/Downhole Tools

**Stephen Midgley**
Operations Superintendent

**Erik Moortgat**
Chemistry Laboratory

**Chieh Peng**
Assistant Laboratory Officer

**Vincent Percuoco**
Chemistry Laboratory

**Alyssa Stephens**
Publications Specialist

**Kerry Swain**
Logging Engineer

**Steven Thomas**
Marine Computer Specialist

**Rui Wang**
Applications Developer

# Abstract

International Ocean Discovery Program Expedition 367 is the first of two consecutive cruises that form the South China Sea Rifted Margin program. Expeditions 367 and 368 share the common key objectives of testing scientific hypotheses of breakup of the northern South China Sea (SCS) margin and comparing its rifting style and history to other nonvolcanic or magma-poor rifted margins. Four primary sites were selected for the overall program: one in the outer margin high (OMH) and three seaward of the OMH on distinct, margin-parallel basement ridges. These ridges are informally labeled A, B, and C within the continent–ocean transition (COT) zone going from the OMH to the steady-state oceanic crust of the SCS. The main scientific objectives include

1. Determining the nature of the basement within critical crustal units across the COT of the SCS that are critical to constrain style of rifting,
2. Constraining the time interval from initial crustal extension and plate rupture to the initial generation of igneous ocean crust,
3. Constraining vertical crustal movements during breakup, and
4. Examining the nature of igneous activity from rifting to seafloor spreading.

In addition, sediment cores from the drill sites will provide information on the Cenozoic regional tectonic and environmental development of the Southeast Asia margin.

Expedition 367 successfully completed operations at two of the four primary sites (Site U1499 on Ridge A and Site U1500 on Ridge B). At Site U1499, we cored to 1081.8 m in 22.1 days, with 52% recovery, and then logged downhole data from 655 to 1020 m. In 31 days at Site U1500, we penetrated to 1529 m, cored a total of 1012.8 m with 37% recovery, and collected log data from 842 to 1133 m. At each site we drilled to reach the depth of the main seismic reflector (acoustic basement), which prior to the expedition had been interpreted to be crystalline basement. Our objective was to determine which lithospheric layer constitutes the basement of the COT and whether there was middle or lower continental crust or subcontinental lithospheric mantle exhumed in the COT before the final lithospheric breakup. At Site U1499, coring ~200 m into the acoustic basement sampled sedimentary rocks, including early Miocene chalks underlain by pre-Miocene polymict breccias and poorly cemented gravels composed of sandstone pebbles and cobbles. Preliminary structural and lithologic analysis suggested that the gravels might be early synrift to prerift sediment. At Site U1500, the main seismic reflector corresponds to the top of a basalt sequence at ~1379.1 m. We cored 149.90 m into this volcanic package, recovering 114.92 m (77%) of sparsely to moderately plagioclase-phyric basalt comprising numerous lava flows including pillow lavas with glass, chilled margins, altered veins, hyaloclastites, and minor sediment. Preliminary geochemical analyses show that the basalt is tholeiitic. We speculate that the basalt might belong to the very early stage of magmatism prior to steady-state seafloor spreading (known as an "embryonic ocean" regime).

Sampling of the Pleistocene to lower Miocene sedimentary section at Sites U1499 and U1500 was not continuous for two reasons. First, there was extremely poor recovery within substantial intervals interpreted to be poorly lithified sands. Second, we chose to drill down without coring in some sections at Site U1500 to ensure sufficient time to achieve this site's high-priority deep objectives. Nevertheless, the upper Miocene basin sequence, consisting of interbedded claystone, siltstone, and sandstone, is continuous on seismic reflection profiles, and can be correlated between the two sites using both seismic reflectors and biostratigraphy. Together with results from other holes previously drilled in the SCS, these samples will help to constrain changes in paleoceanographic conditions during the Miocene in this part of the SCS basin.

# Introduction

The South China Sea (SCS) margin (Figure **F1**) is an accessible and well-imaged location where drilling of synrift sediment and underlying basement will provide key constraints on the processes of rifting and eventual rupturing of the continental lithosphere during breakup at a highly extended rifted margin. Expedition 367/368 was based on International Ocean Discovery Program (IODP) drilling Proposals 878-CPP, 878-Add, 878-Add2, and 878-Add3. This project was implemented as a single science program with 114 days of drilling operations spread across two IODP expeditions as outlined in the Expedition 367/368 *Scientific Prospectus* (Sun et al., 2016b). Two expeditions were required to drill four deep-penetration sites in a transect across the margin. Three sites targeted acoustic basement in the continent–ocean transition (COT) and one site targeted late prerift to synrift sequences on the landward side of the transect.

Although the primary focus of this drilling expedition is to discriminate between possible models for rifting and plate rupture, the drilling, along with results from Ocean Drilling Program (ODP) Leg 184 and IODP Expedition 349, addresses a secondary objective of providing much improved constraints on the Cenozoic development of the southeast Asian margin as recorded within the South China Sea Basin. The strategy for Expedition 367/368, however, was entirely optimized to achieve the primary deep basement coring and logging objectives.

# Background
## Global questions regarding formation of rifted margins

The Ocean Drilling Program (1985–2003) made a major effort along the rifted margins of the North Atlantic to understand the processes of continental breakup (ODP Legs 103, 104, 149, 152, 163, 173, and 210). This has resulted in the recognition of two end-members of rifted margins (see summary of observations in Sun et al., 2016a, 2016b):

Volcanic rifted margins: The examples are characterized by massive igneous activity in a relatively short period of time (~1–3 million years) during breakup and initial seafloor spreading. The pair of conjugate margins of Greenland and northwest Europe is a type example. In these locations, the asthenospheric mantle may have been anomalously hot (e.g., mantle plumes), leading to thermal weakening of the continental lithosphere followed by rapid plate rupture.

Magma-poor rifted margins: The examples that have been drilled so far show hyperextension of the continental crust, with tectonic extension eventually leading to exhumation and serpentinization of the subcontinental mantle lithosphere. The Newfoundland and Iberia conjugate margin, where serpentinite occupies a broad zone within the COT zone, is an example of this type. The introduction of water into the subcontinental lithospheric mantle is interpreted to have taken place through deep, crust-cutting faults. This caused serpentinization that profoundly weakens the mantle lithosphere and facilitates plate rupture. The subsequent ultraslow spreading led to formation of additional serpentinite on the seafloor

(e.g., Dick et al., 2003) until higher spreading rates allowed sufficient magma production for normal oceanic crust to form.

Other examples of highly extended rifted margins have been identified in seismic reflection data elsewhere (e.g., Brune et al., 2017; Doré and Lundin, 2015). However, it is not known if serpentinized mantle plays a critical role in all cases. Modeling by Huismans and Beaumont (2008, 2011) suggests several scenarios for the formation of rifted margins in the absence of anomalously hot asthenospheric mantle. One scenario (Type I of Huismans and Beaumont, 2011) is the Iberia-Newfoundland–type margin described above. In this case, lithospheric thinning initially occurs in the (upper) crust, with extensional faults profoundly thinning the continental crust (hyperextension), eventually reaching the mantle and causing serpentinization (Whitmarsh et al., 2001; Pérez-Gussinyé and Reston, 2001; Pérez-Gussinyé et al., 2006; Reston, 2009; Sutra and Manatschal, 2012). Alternative modeling scenarios suggest that final plate rupture can occur without exhumation of the subcontinental mantle and associated serpentinization during breakup (Figure **F2**).

It is not easy to determine if tectonic exhumation reached the subcontinental mantle using seismic data alone; drilling control is needed. However, only one of the highly extended margins has been drilled (the conjugate Iberia-Newfoundland margins mentioned above). The highly extended northern margin of the SCS is an excellent location for drilling to constrain seismic interpretations of the style of rifting.

## Geological setting

The SCS is a modestly sized young ocean basin that formed along the eastern boundary of the Eurasian plate during mid- to late Cenozoic time (Figure **F1**). Expeditions 367 and 368 cored and logged a transect of drill sites across the COT in the northern SCS. The seafloor in this region is thought to have first formed at ~32–30 Ma with a later expansion of seafloor spreading into the southwest SCS (Briais et al., 1993; Barckhausen and Roeser, 2004; Li et al., 2012a, 2012b; Franke et al., 2013).

The continental crust that was rifted to form the SCS was accreted to the Asian margin during the Mesozoic (Zhou and Li, 2000; Zhou et al., 2008; Li et al., 2012a, 2012b). Within ~80 million years, this relatively young continental lithosphere underwent extensive rifting during the Paleogene, most likely from the early Eocene (~45 Ma). Seafloor spreading in the SCS started in the early Oligocene, with the oldest interpreted magnetic anomaly in the vicinity of the drilling transect being Anomaly C11 (~30 Ma) or C12n (~31 Ma) (Briais et al., 1993; Li et al., 2013, 2014; Franke et al., 2013). These studies concluded that seafloor spreading ceased within the middle Miocene. The initial half-spreading rate was ~3.6 cm/y, which then dropped to 1.2 cm/y and stopped by 15 Ma (Li et al., 2014). The initial spreading rate in the SCS basin therefore provides for different geodynamic boundary conditions than the ultraslow spreading scenario of the Iberia-Newfoundland margin. Subduction of the eastern part of the SCS basin started at or before ~15 Ma along the Manila Trench (Li et al., 2013). However, this essentially postspreading subduction did not affect the northern SCS margin. For a more complete review of the regional setting and tectonic development of the SCS, see Shi and Li (2012), Li et al. (2013), Sun et al. (2014), and Franke et al. (2013).

The Expedition 367/368 drilling transect is located ~50 km west of IODP Site U1435 (Figures **F1**, **F3**, **F4**) (Li et al., 2015c) along the northern SCS margin. The oldest seafloor spreading magnetic anomaly identified on this specific part of the northern SCS margin

is most likely no older than Anomaly C11 (~30 Ma) (i.e., slightly younger by ~1–2 million years than further east along the northern SCS margin where Anomaly C12 is interpreted to be present). This segment of the SCS margin exhibits a broad zone (~150–200 km) of across-margin crustal stretching and extension prior to breakup. Within this zone, seismic data (Figures **F3**, **F4**, **F5**) exhibit three distinct ridges (A, B, and C) along the seaward margin of the COT as well as an outer margin high (OMH), each of which was targeted by this drilling transect (Figure **F5**).

We define the COT as the broad (100–150 km) zone from moderately thinned continental crust (~20 km thick) to the thin (~6 km) crust below the ocean basin (Figure **F5**). We refer to the continent/ocean boundary (COB) as the much narrower zone in which the outermost, highly thinned continental lithosphere is replaced seawards by crust that formed within a narrow zone at a spreading ridge in a steady-state fashion. The latter can include continuous tectonic exhumation of rising lithospheric mantle (e.g., Dick et al., 2003), accretion of normal igneous oceanic crust, or a mixture of these two processes.

Clear Mohorovicic seismic discontinuity (Moho) seismic reflections (Figure **F5**) show distinct thinning of the continental crust across the COT with a thickness of ~6 km around the interpreted COB. Separate layers hypothesized to be upper, middle, and lower crust are present within the landward part of these seismic profiles. The lower crust is acoustically transparent and can be as thin as only ~6 km. Lower crust with a similar thickness and seismic appearance is reported from the northeastern SCS margin (McIntosh et al., 2013, 2014; Lester et al., 2013). The seaward continuation of this crustal layering into the COB zone is, however, ambiguous.

The upper crust shows numerous extensional, low-angle detachment faults soling out at midcrustal level. This fault system generated a number of deep half-grabens filled with synrift sediment, subsequently covered by postrift sediment. The synrift sediment is topped by a breakup unconformity (T70 in Figure **F5**). Industry data (distant wells with only cuttings and log data) and Site U1435 results suggest a break-up unconformity age of ~32 Ma, but this needed to be verified by coring data (Figure **F5**). This unconformity is interpreted to reflect the end of the main crustal extension. However, the time of crustal extension is not necessarily synchronous across the margin and could be younger toward the outer margin. A younger, widely distributed unconformity (T60) is also shown in Figure **F5** and likely reflects the development of a shallower continental margin and a true, deep oceanic basin. The unconformity may correspond to a hiatus at ~23 Ma found at ODP Site U1148 (Wang, Prell, Blum, et al., 2000) and at site U1435; it is approximately synchronous with a southward jump of the SCS spreading axis (Briais et al., 1993).

The distinct OMH of seismic Line 1555 is also well developed on seismic Line 15ecLW8 (see figure F5 in Sun et al., 2016b). These basement structures are quite reminiscent of the structure drilled at Site U1435, but here they are located farther inland of the interpreted magnetic Anomaly C11 than at Site U1435 (Figure **F3**). This would be consistent with an interpretation of a wider zone of significant crustal extension within this westerly margin segment compared to that of Site U1435 farther east.

Seaward of the OMH, seismic data (e.g., Figures **F4**, **F5**) show the presence of the three basement Ridges A, B, and C within and south of the COT, close to but landward of the interpreted boundary between continental and oceanic lithosphere (COB). The seismic images of these basement highs are different from those of the OMH fault blocks. In particular, Ridge A is for the most part more

dome-like, with neither normal faults nor clearly developed synrift half-grabens on the landward-facing part of these structures (Site U1499 and proposed alternate sites). Note that magnetic Anomaly C11 is projected to almost overlap the seaward part of Ridge A. Excluding sediment, the crust below this outermost basement high is only ~6.4–8 km using ocean-bottom seismometer (OBS) velocity constraints of Yan et al. (2001), Wang et al. (2006), and Wei et al. (2011). Seaward of Ridge A, the crust has a fairly uniform thickness of ~6 km, which could be consistent with oceanic crust (Yan et al., 2001). However, the existence of highly thinned continental crust or serpentinized mantle cannot be ruled out. The nature of the basement within these three ridges is key to constrain tectonic models for the margin development.

In the general summary of key structures (Figure **F5**; see also Figure F6B in Sun et al., 2016b), the normal faults of the upper, brittle crust sole out within a main detachment zone located above or within the middle crust. This suggests decoupling between upper and lower crustal extension. The lower crust within the COT may thicken oceanward (lower crustal flow?), but this is not well imaged beneath the COB. Likewise, seismic imaging of the low-angle faults and detachments within the landward part of the COT cannot with confidence be traced through the COB, leaving widely different interpretations of the nature of the COB possible.

One possibility is that the main detachment zone itself became exhumed during final breakup. This would imply that the former position of the main detachment zone actually was above the outermost basement high (i.e., Site U1499 at Ridge A) and that either lower crust or serpentinized mantle is present within Ridge A. Alternatively, if the main detachment underlies Ridge A, one would expect Ridge A to comprise upper crustal material.

Alternatively, the "Moho" in this zone below the COT may be a serpentinization front. Sampling of basement on Ridge A, such as at site U1499, is therefore pivotal to constrain crustal structure and critical aspects of the extension process.

Both Ridges B and C consist of fault blocks rotated landward along seaward-dipping normal faults. Some of these faults may be seismically traced to the base of the crust. Ridge B shows seismic features along strike and within the uppermost crust that could be consistent with a volcanic origin. However, these features could also be consistent with a rotated fault block of upper continental crust (i.e., a distal extensional rider of upper-plate origin), in which case there might be prerift sediment below the breakup unconformity defining the top of acoustic basement at Ridge B. The possibility of Ridge B representing exhumed lower crust or mantle is less likely. Ridge C in many ways is seismically similar to Ridge B. However, an apparent reversed magnetic anomaly strongly suggests that this ridge represents igneous ocean crust.

Sampling the basement at Ridges A, B, and C is therefore essential for Expeditions 367/368 to distinguish between different tectonic models for breakup along highly extended margins. Ridges A and B help to constrain the style of rifting. In contrast, Ridge C is assumed to represent the early igneous crust and will address another key objective of Expeditions 367 and 368: to constrain the nature of early oceanic crust formation. This includes determining how quickly after breakup a robust igneous system was established, what mantle source is involved (e.g., wet/dry, temperature), under what conditions mantle melting occurs (degree and depth of melting), and the contribution of continental crustal contamination.

# Expedition objectives

This two-expedition drilling transect across the SCS margin (Figure **F1**) was implemented to understand the processes of rifting, eventual rupturing of the continental crust, and the onset of igneous oceanic crust at a highly extended rifted margin. Four primary and sixteen alternate drill sites across a 150–200 km wide well-imaged COT zone were targeted as part of the overall program (see Sun et al., 2016b). Expedition 367 set out to conduct operations at two of the primary sites (U1499, U1500) (Figures **F1**, **F2**, **F3**, **F4**, and **F5**).

The most landward site (U1501), located on the OMH shown in Figure **F4**, will target late prerift to synrift sediment within a rotated fault-block overlain by postrift sediment. Data from the site will constrain the timing of rifting, rate of extension, and rifting environment, including subsidence prior to breakup. However, to constrain how deeply the continental crust was exhumed during breakup, we need to know the nature of the basement at Ridges A and B within the COT. Ridge C, at the seaward end of the COB, is assumed to be the earliest igneous crust and will constrain the nature of the earliest oceanic crust formation.

The postbreakup sedimentary sections from the developing ocean basin will constrain the late synrift and postrift subsidence history of the margin. This sediment, when combined with previous ODP and IODP cores, will provide a basis for documenting the Neogene paleoclimate and environmental changes within the larger southeast Asian region.

## Drilling, coring, and logging strategy

Operations for this SCS rifted margin science program were distributed across Expeditions 367 and 368 and were designed to core and log through thick sediment sections and, significantly, into underlying basement. We intended that the overall operational approach at each site would be similar and consist of two holes per site (Figure **F6**).

The first hole at each site was to be cored with the advanced piston corer (APC) and extended core barrel (XCB) systems to ~650 m, and then we would log the hole with the triple combo and Formation MicroScanner (FMS)-sonic tool strings. This APC/XCB hole was also to document borehole and formation conditions to help determine the length of casing to be drilled into the seafloor in the second hole. All full APC cores were intended to be oriented and formation temperature measurements made using the advanced piston corer temperature tool (APCT-3).

The second hole at each site was designed to begin by drilling in a seafloor reentry system with casing extending to ~650 mbsf or to the depth determined in the first hole. This was intended to enhance our chances of achieving our deep coring and logging objectives. Coring using the rotary core barrel (RCB) system would then extend from the base of the casing, through the sediment, and into the underlying basement. Multiple pipe trips to install new RCB bits were to be made as required. Upon completion of the coring objectives, the RCB bit was to be dropped either in the bottom of the hole or on the seafloor so that downhole wireline log data could be collected. For this deeper logging, we planned to use the triple combo and FMS-sonic tool strings as well as the Versatile Seismic Imager (VSI) tool string to conduct check shots.

During Expedition 367, we had to modify this general operational plan in response to borehole conditions and the need to focus our operations time to achieve our highest priority basement objec-

tives. The planned versus implemented operations are shown in Figure **F6**.

The pilot hole, U1499A, consisted of APC/XCB coring until refusal. In the first (pilot) hole at Site U1500, we washed down without coring within the limits of safety approval and the requirements to identify appropriate locations for setting casing in the subsequent hole. We also decided to not collect downhole log data in either of these pilot holes partly due to poor borehole conditions that we thought would not yield good data as well as to focus more time on the deeper core and log objectives.

For the primary, deep-penetrating, cased holes at each site (Holes U1499B and U1500B), we set as much casing as possible (651 m in Hole U1499B and 842 m in Hole U1500B) to keep the upper part of the hole in stable condition for drilling and to enhance our ability to clean cuttings out of such deep holes. Casing was drilled into the seafloor to total depth as a single step at each location to minimize hole disturbance as well as to save time. We then drilled and cored using the RCB below the casing until we reached the basement (Hole U1500B) or until hole conditions prevented further coring (Hole U1499B). We collected downhole logging data in the deep penetration hole at each site.

# Site summaries
## Site U1499

Site U1499 is located on basement Ridge A within the SCS COT zone ~60 km seaward and southeast of the OMH. The goal of drilling here was to core through the sediment to sample the basement rocks and thus determine basement age and lithology. This would provide a test of different possible models for the processes and rheology controlling the extension and ultimate breakup of the continent. Ridge A was expected to have basement of either upper continental crust, lower continental crust, or mantle rocks, which might or might not have been serpentinized. Coring and drilling also constrain the postrift history by determining the age, water depth, and subsidence rates of the overlying sedimentary packages.

We conducted operations in two holes at Site U1499 (proposed Site SCSII-14A). Hole U1499A is located at 18°24.5698′N, 115°51.5881′E in a water depth of 3760.2 m. In Hole U1499A, APC/XCB coring penetrated from the seafloor to 659.2 m and recovered 417.05 m (63%). Hole U1499B is located at 18°24.5705?N, 115°51.5990?E in a water depth of 3758.1 m. We installed casing in Hole U1499B to 651 m followed by RCB coring that penetrated from 655.0 to 1081.8 m and recovered 150.64 m (35%). Coring terminated in gravel before deteriorating drilling conditions prevented further penetration; no crystalline basement was encountered. Despite challenging conditions in the lowermost part of Hole U1499B, two successful wireline logging runs were conducted from 652 to 1020 m.

### Lithostratigraphy

The cored sediment at Site U1499 is divided into nine lithostratigraphic units (Figure **F7**). Lithostratigraphic Unit I is a 48.85 m thick middle–upper Pleistocene sequence of dark greenish gray bioclast-rich clay with thin clayey silt and sand interbeds. Fining-upward silty and fine sand intervals are abundant and interpreted as turbidite sequences. Four thin (2–7 cm) ash layers were identified in Unit I; none are observed in the deeper units. Unit II (48.85–100.04 m) is a 51.19 m thick lower–middle Pleistocene sequence of interbedded greenish gray clay-rich calcareous ooze and dark greenish gray nannofossil-rich clay. Synsedimentary deformational structures such as folds, microfaults, and inclined beds are well developed in the sediment of this unit, which is interpreted as a slump deposit. This unit is underlain by Unit III (Pliocene–middle Pleistocene), which is divided into Subunits IIIA (100.04–181.80 m) and IIIB (181.80–333.65 m). The 233.61 m of Unit III is dominated by dark greenish gray clay with very thin to thin clayey silt and calcareous sand intervals. Subunit IIIA contains clayey silt layers that are very thin (<1 cm), whereas Subunit IIIB has abundant thin (2–5 cm) clayey silt layers and an overall increase in nannofossil and foraminifer content. Unit IV (333.65–404.90 m) is a 71.25 m thick sequence of upper Miocene–Pliocene dark greenish gray silty sand with clay interbeds. Recovery is very low throughout the section, but the recovered intervals suggest that the unit may contain unconsolidated to weakly consolidated sand.

Unit V (404.90–469.45 m) is a 64.55 m thick sequence of upper Miocene dark greenish gray clay with mostly thin (<5 cm) clayey silt and foraminifer sand interbeds. Drilling disturbance, in the form of biscuiting, increases significantly in this unit. Similar to Unit IV, recovery in Unit VI (469.45–618.30 m) is also very low. The recovered intervals in this unit include upper Miocene dark greenish gray silty sand with clay interbeds. Unit VII (618.30–761.70 m) is mainly composed of upper Miocene dark greenish gray to dark gray sandstone and claystone with siltstone interbeds. Lithification increases sharply downhole from the top of this unit, although sections with very low recovery are inferred to be nonlithified sand. Unit VIII (761.70–929.02 m) comprises a 167.32 m thick interval of Miocene reddish brown to reddish gray claystone and clay-rich chalk. Based on the abundance of calcareous material, this unit is divided into two subunits. Subunit VIIIA (761.70–892.10 m) contains lower–upper Miocene dark reddish brown claystone with siltstone and foraminifer sandstone interbeds, whereas Subunit VIIIB (892.10–929.02 m) is composed of lower–middle Miocene reddish brown to reddish gray clay-rich nannofossil chalk and clay-rich chalk. In the lowest part of Subunit VIIIB, abundant brownish black iron-manganese nodules occur within reddish brown nannofossil-rich claystone.

Unit IX (929.02–1081.80 m) is readily distinguished from the overlying units by containing pre-Miocene sandstone, claystone, matrix-supported breccia, and gravel. This unit is 152.78 m thick and comprises three subunits. Subunit IXA (929.02–933.28 m) is defined by brownish and greenish gray sandstone and breccia. Subunit IXB (933.28–933.35 m) is defined by dark gray matrix-supported breccia in Core 367-U1499B-30R. Subunit IXC (933.35–1081.80 m) contains gray to dark gray gravel with silty sand intervals. The cores in Subunit IXC are completely fragmented and were recovered as pebbles and cobbles. In general, the pebbles and cobbles are recycled sedimentary rocks (such as sandstones) that contain a variety of individual lithic components including igneous, sedimentary, and metamorphic grains. However, the matrix that likely surrounded these cobbles and pebbles was not recovered; we inferred that the matrix is poorly consolidated and washed away by the drilling process.

### Structural geology

The tilting of sedimentary beds and deformation structures observed at Site U1499 are limited to lithostratigraphic Units II, VII, VIII, and IX. The folds, faults, and tilted beds observed in Unit II are related to two slump events that reworked older sediment between younger Units I and III. Tilted beds and faults with slickensides are observed in Unit VII and VIII. These faults are linked to compaction processes of the clays, and the tilted beds are associated with sandy layers. Unit IX is divided into three subunits. In Subunit IXA,

tilted beds as well as a downhole increase in clast size, angularity, and proportion of clasts are observed. The matrix-supported breccia of Subunit IXB exhibits no clear deformation structure or tilted sedimentary bedding. Some of the sandstone and breccia clasts in Subunit IXC exhibit veins and fractures. These clasts were transported before sedimentation; therefore, their veins and fractures must have originated in some previous tectonic event.

### Biostratigraphy

All core catcher samples at Site U1499 were analyzed for calcareous nannofossil and foraminiferal content, and additional samples were taken from the split-core sections when necessary to refine the ages. Preservation of microfossils varies from poor to very good, and total abundance varies from barren to abundant. Although samples exhibit some degree of reworking, 28 biostratigraphic datums are recognized, revealing that we recovered an apparently continuous succession of Oligocene to Pleistocene age, spanning nannofossil Zones NN5−NN21 and foraminifer Zones M4/M3 to Subzone PT1b. The Pleistocene/Pliocene boundary is located between Cores 367-U1499A-20X and 27X, and the Pliocene/Miocene boundary is located between Cores 31X and 43X. Sedimentation rates varied from ~8 cm/ky in the late Miocene to the early Pliocene and ~5 cm/ky in the early Pliocene to the early Pleistocene to ~13 cm/ky in the middle−late Pleistocene. Extremely low sedimentation rates (~1 cm/ky) occurred in the early to late Miocene during deposition of Unit VIII. The succession of Subunit IXA contains late to early Oligocene microfossils with calcareous nannofossils that are well preserved and abundant, whereas foraminifers are sorted or sparse. This indicates that Unit IX is probably transported and reworked.

### Paleomagnetism

Paleomagnetic analysis was conducted on both archive-half sections and discrete samples from the working half. The archive-half sections were measured with the pass-through superconducting rock magnetometer (SRM) with demagnetization steps at 5, 15, and 25 mT. The discrete samples were subjected to alternating field (AF) and thermal demagnetization, and remanence was measured on the spinner magnetometer. We adopted a combination of stepwise AF and thermal demagnetization steps to fully demagnetize the discrete samples and obtain the characteristic remanent magnetization (ChRM).

Variations in the natural remanent magnetization (NRM) intensity are well correlated to observable changes in lithology and magnetic susceptibility; for example, the low NRM intensity at ~60 m (Core 367-U1499A-7H) agrees with the carbonate-rich slump in which magnetic susceptibility values are also low. Drilling-induced remanence was identified and removed in most core sections at AF treatments of 15 mT. In addition, magnetic mineral variations were observed from the demagnetization behavior. From Core 367-U1499B-12R downhole, the drilling overprint becomes stronger and hard to remove with the relatively low AF steps used on the archive-half sections, whereas AF treatments up to 200 mT and temperatures up to 675°C could not fully demagnetize the discrete samples. These characteristics confirm the presence of hematite and magnetite.

We constructed a Site U1499 magnetostratigraphy based on the interpretation of the raw paleomagnetic data with stable and clear demagnetization behaviors. Core orientation from 0 to 162 m was used to correct the declinations; downhole from there, our interpretation is based only on inclination data. When making comparisons

to the standard geomagnetic timescale, we obtained several tie points. For example the Brunhes/ Matuyama Chron boundary (0.78 Ma) is at ~110 m, and the middle of Subchron C2An.3n is placed at ~260 m. We thus conclude that the middle/early Pleistocene boundary (0.78 Ma) is at ~110 m, the early Pleistocene/late Pliocene boundary is at ~220 m, the late/early Pliocene (3.6 Ma) boundary is at ~260 m, and early Pliocene/late Miocene boundary (5.33 Ma) is at ~370 m.

### Geochemistry

Geochemical analyses were conducted for headspace gas safety monitoring; quantification of sediment $CaCO_3$, organic carbon, and nitrogen content; and interstitial water characterization. Calcium carbonate contents vary between 0.4 and 82 wt%, with higher values of >20 wt% corresponding to intervals of nannofossil/foraminifer ooze or chalk. Total organic carbon (TOC) contents mostly range from ~0 to ~ 1.0 wt%. TOC decreases gradually downhole from 1.0 to 0.3 wt% in the uppermost 110 m corresponding to the base of the sulfate reduction zone, reflecting active degradation of sedimentary organic matter. The TOC to total nitrogen molar ratio (C/N) is mostly <8, indicating that TOC is derived dominantly from a marine source.

Hydrocarbon monitoring shows headspace gas consistently approaching zero throughout the site. Relatively higher methane contents of ~tens to 6000 ppmv occur across the ~100–250 mbsf interval, just below the sulfate reduction zone. The overall low methane content indicates limited microbial methanogenesis likely caused by low TOC contents (<0.3 wt%) deeper than 110 mbsf.

We obtained 58 interstitial water samples from Hole U1499A. The inorganic geochemistry of interstitial water is controlled by the remineralization of organic matter as well as carbonate and clay diagenesis. The sediment rapidly becomes suboxic, as indicated by a Mn peak of ~120 µM at ~6 m. Sulfate reduction coupled with sedimentary organic matter degradation occurs until ~110 m, with near-complete depletion until 257 m before increasing slowly to 16.9 mM at the bottom of Hole U1499A. The interval of near-complete sulfate consumption is also marked by pronounced high Ba concentrations >50 µM, suggesting the dissolution of barite (BaSO$_4$). The peak alkalinity and steady increase in $NH_4^+$ and $Br^-$ in the upper 110 m are consistent with progressive remineralization of sedimentary organic matter. The gradual decrease in $Ca^{2+}$ shallower than 80 m suggests active authigenic carbonate precipitation triggered by sulfate reduction. A subsequent downhole increase in $Ca^{2+}$ and $Sr^{2+}$ is likely caused by biogenic carbonate dissolution and recrystallization. Nearly parallel downhole decreases in $Mg^{2+}$ and $K^+$ are mostly driven by clay mineral cation exchange and/or clay mineral authigenesis. The lower $Cl^-$ and $Na^+$ concentrations compared to those of seawater at the bottom of the Hole U1499A are mostly driven by the smectite-illite transformation. Elevated Si concentrations of 700−820 µM from the seafloor to 45 m suggest active dissolution of biogenic silica.

### Petrophysics

At Site U1499, measurements of $P$-wave velocity, bulk density, magnetic susceptibility, and natural gamma radiation (NGR) were made on whole-round cores, and additional measurements were made on split cores and discrete samples, including thermal conductivity; caliper $P$-wave velocity (PWC); porosity; and bulk, dry, and grain density. In general, bulk density, $P$-wave velocity, and thermal conductivity increase with depth, whereas porosity decreases with depth as a result of compaction and lithification. How-

ever, some properties, such as NGR or magnetic susceptibility, show local variations related to the specific lithology. The soft sediment in the upper 100 m shows rapid compaction with depth, marked by a decrease in porosity and increase in bulk density and thermal conductivity. Four thin volcanic ash layers in the uppermost 50 m are marked by peaks in magnetic susceptibility. The mass transport deposit (48.85–100.04 m) displays low magnetic susceptibility and low NGR counts, reflecting the high carbonate content of the calcareous ooze. Below these layers downhole to ~890 m, physical properties show small variations; bulk density, *P*-wave velocity, and thermal conductivity gradually increase, whereas porosity decreases with depth. The NGR and magnetic susceptibility data in this interval do not show much variation. From 830 to 930 m, we observed a general decrease in magnetic susceptibility values and NGR counts where densities increase slightly and *P*-wave velocities increase significantly from 2200 to 2900 m/s. These variations are associated with a significant increase in the carbonate content in the Subunit VIIIB chalks. The cobbles and pebbles in the deepest part (930–1080 m) show large variations in NGR, bulk density, and *P*-wave velocity and very low magnetic susceptibility.

**Downhole measurements**

Two downhole logging tool strings were run in Hole U1499B, a modified triple combo (sonic velocity, NGR, bulk density, resistivity, and caliper) tool string and the FMS-sonic tool string (FMS resistivity images and calipers and NGR). We added the velocity tool to the first tool string because sonic velocities were needed for an accurate prediction of basement depth for the subsequent Site U1500 as well as to better constrain core-log-seismic correlation. We also did not know if hole conditions would allow a second logging run. Although stable borehole conditions in Hole U1499B allowed the second FMS logging run, we did not attempt a check shot due to time constraints and concerns about hole stability. Borehole conditions from the bottom of the casing at ~651 m to the bottom of Hole U1499B at ~1020 m were generally good, with measured diameters from ~10 to 16 inches. Washout zones are observed from 670 to 710 m, which corresponds to an interval of very low core recovery, as well as from 830 to 920 m, affecting quality of the log data in these intervals. Log and core data generally show a good agreement. Downhole logging provided information in zones of poor core recovery in Hole U1499B. The log data from 726 to 739 m exhibits high NGR values and low bulk densities and *P*-wave velocities, whereas the data from 820 to 840 m is characterized by a sharp increase in bulk densities, a slight increase in *P*-wave velocities, and an abrupt decrease in NGR values compared to average values above and below these depths. The Subunit VIIIB chalks (~890–930 m) display a sharp decrease in NGR and an increase in bulk density and P-wave velocity with depth, as well as only small variations in resistivity. Deeper than 930 m, bulk densities, *P*-wave velocities, and resistivities show large variability, in part because of the presence of cobbles and pebbles. The quality of the acquired FMS images is strongly influenced by hole-diameter variations; they generally show alternating smooth and patchy textures with contrasting resistivity values marking horizontal to slightly tilted bedding downhole to 930 m. The deepest layers of sandstones, breccias, and gravels show highly variable and oblique textures on the FMS images, possibly reflecting the varied orientation of the gravel clasts or the presence of faults and fractures in the gravel or the matrix. In general, the velocities measured with the sonic velocity logging tool match the PWC measurements taken with the caliper on the split cores. Six in situ formation tem-

perature measurements were made in Hole U1499A and give a geothermal gradient of 93°C/km. The estimated heat flow is 110 mW/m$^2$, a value in agreement with the general heat flow of the area.

**Correlation to seismic data**

We used downhole log data and physical property measurements on cores and samples as well as other available data to correlate Site U1499 data with the available seismic reflection profiles. We also used the Site U1499 density and sonic velocity data to create synthetic seismograms that provided additional constraints on the correlation. Log sonic velocities and PWC velocities are in very good agreement except for the deepest breccias and gravels (deeper than ~930 m) where measurement on individual pebbles leads to an overestimate of the velocity in the formation. For seismic correlation, we use the PWC and density values from moisture and density (MAD) and gamma ray attenuation (GRA) measurements from Hole U1499A (0–655 m), whereas below we used the downhole logging velocity and density data. We used a constant velocity of 2100 m/s in the low-recovery zones (333–406 and 531–561 m), interpreted to be sandy layers, based on the downhole logging velocity values measured at greater depth. The comparison of the time-depth relation (TDR) obtained for Site U1499 to those for ODP Site 1148 as well as IODP Sites U1431 and U1433 shows substantial agreement, except for the Site 1148 TDR, which shows higher velocities in the deeper layers. The comparison between the seismic reflectors and the variations in physical properties and lithology characteristics using the computed Site U1499 TDR shows a good correlation between the main upper reflectors and the poor-recovery sandy intervals. However, the main physical property changes related to the top of the deep gravel layer do not correlate to the reflector observed at ~5.9 s in the seismic profile.

# Site U1500

Site U1500 is located on basement Ridge B and is the most seaward site that Expedition 367 drilled within the SCS COT zone. Ridge B is located ~80 km seaward of the OMH and ~20 km seaward of Ridge A, where Site U1499 was drilled. The goal of drilling here was to sample and log the lowermost sediment and underlying basement rocks to determine basement age and lithology of the COT or embryonic oceanic crust. This would provide a test of different possible models for the processes and rheology controlling the breakup of the continent. Ridge B was expected to have basement of either upper continental crust, lower continental crust, mantle rocks, or oceanic crust. The coring and logging would also constrain the history of the region after rifting by determining the age, water depth, and subsidence rates of the overlying sedimentary packages.

We conducted operations in two holes at Site U1500 (proposed Site SCSII-8B). Hole U1500A is located at 18°18.2762′N, 116°13.1916′E in a water depth of 3801.7 m. In Hole U1500A, we drilled without coring from the seafloor to 378.2 m, and then cored with the RCB from 378.2 to 494.6 m and recovered 26.5 m (23%). Thereafter, we drilled without coring from 494.6 to 641.2 m, and cored with the RCB from 641.2 to 854.6 m and recovered 67.2 m (31%).

Hole U1500B is located at 18°18.2707′N, 116°13.1951′E in a water depth of 3801.7 m. After installing casing, we continuously cored the sediment sequence from 846.0 to 1379.1 m (533.1 m cored; 164.7 m recovered; 31%), and then continuously cored 149.9 m into the underlying basalt from 1379.1 to 1529.0 m (114.92 m recovered;

77%). This made Hole U1500B the eighth deepest hole that the R/V *JOIDES Resolution* has drilled in ODP/IODP history. Three downhole logging strings were run in Hole U1500B from 842 to 1133 m.

### Lithostratigraphy

The cored sediment at Site U1500 is divided into eight lithostratigraphic units (Figure **F8**). The uppermost 378.2 m of sediment was drilled without coring. Lithostratigraphic Unit I (378.2–410.0 m) is a 31.8 m thick upper Miocene sequence of greenish gray heavily bioturbated clay with silt and sandy silt interbeds. Some of the clay intervals are nannofossil rich. Structure in the clay is mostly massive, but parallel laminations occur in the silt and sandy silt interbeds. Unit II (410.0–494.6 m) is an upper Miocene sequence of interbedded dark greenish gray clay and silt. Recovery was very low for this unit (~8%), which may indicate a change in lithology (e.g., increased abundance of nonlithified sands). This unit is underlain by another interval drilled without coring (494.6–641.2 m).

Unit III (641.2–892.4 m) is defined by upper Miocene interbedded claystone, siltstone, and sandstone. Many of the siltstone and sandstone intervals are organized into a variety of massive and stratified beds that include sedimentary structures such as parallel laminations, cross-stratification, and contorted strata. There are also several massive beds of sandstone that contain pebble-sized mud clasts. The well-organized coarser intervals fine upward into more massive claystone intervals and are interpreted as turbidite sequences. Several of the stratified beds are composed of foraminifer tests.

Unit IV (892.4–1233.3 m) also had very low recovery (15%). This unit is composed of upper Miocene very dark greenish gray to dark gray sandstone with dark brown to very dark gray claystone and siltstone intervals. Many of the intervals described in this unit contain interlaminations of silt or sand within a prevailing claystone lithology. Similar to Unit III, sedimentary structures in many of the sandstone and siltstone intervals are interpreted as turbidites. The claystone in some of the cores shows a distinctive color banding, which was observed as a pattern of alternating reddish brown, dark greenish gray, and brownish gray. The color banding appears to be associated with fining-upward grain sizes and varying levels of bioturbation. Sandstone intervals within this unit contain high percentages of potassium feldspar, quartz, plagioclase, and mica minerals, which may have been sourced from granitic rocks exposed along the southern margin of China.

Unit V (middle–upper Miocene) was divided into Subunits VA (1233.30–1272.10 m) and VB (1272.10–1310.98 m) based on the abundance of calcareous material. Subunit VA consists of dark reddish brown, dark greenish gray, and dusky red homogeneous, massive claystone with few sandstone and siltstone interbeds (3–12 cm thick). Subunit VB consists of dark reddish brown, reddish brown, and greenish gray intervals of claystone, nannofossil-rich claystone, claystone with biogenic carbonate, and clay-rich chalk. Intervals of greenish gray color within Subunits VA and VB unit are interpreted as diagenetic alteration.

Unit VI (1310.98–1370.33 m) is composed of middle Miocene dark greenish gray massive silty claystone with biogenic carbonate and dark gray sandstone. Unit VII (1370.33–1379.10 m) comprises a thin (30 cm thick) middle Miocene dusky red claystone. The lowermost 2 cm of this unit has a greenish gray color that marks a sharp horizontal contact with the igneous rocks below in Unit VIII. The pre-middle Miocene basalt in Unit VIII (1379.10–1529.0 m) contains some fractures that are filled with well-lithified claystone. The claystone contains authigenic carbonate, siliciclastic components, and rare nannofossils. The basalt intervals are sparsely intercalated with dusky red claystone, with the basalt/sediment contacts often associated with chilled, glassy margins. Some claystone intervals within the basalt unit show evidence of dolomitization in thin section.

### Igneous petrology

In Hole U1500B, we cored 149.9 m of igneous rocks below the sedimentary section and recovered a total of 114.92 m of basalt. The aphanitic to porphyritic basalts are nonvesicular to moderately vesicular and glassy to hypocrystalline, with the latter ranging from cryptocrystalline to fine grained, making up an aphyric to highly olivine-plagioclase phyric microstructure. These basalts contain numerous 2–5 cm thick chilled margins, many with preserved fresh glass, as well as occasional hyaloclastites with brecciated glass fragments mixed with sediment. The basalts comprise Unit VIII and are divided into two igneous subunits (1a and 1b) according to flow boundaries to distinguish an upper massive lava flow sequence (27.28 m thick) from a lower, predominantly pillow lava flow succession (122.62 m thick) with subordinate thin (<6 m) interbedded lobate, sheet, and massive lava flows. The pillow lobes are well preserved and are separated by chilled, glassy margins (identifying upper and lower chilled margins of individual pillows where possible) and also claystone. Plagioclase phenocrysts are found throughout these basalts with olivine being an occasional phenocryst. Modal abundances of olivine and plagioclase phenocrysts increase downhole, reaching a peak between 1420 and 1470 mbsf. Veins occur throughout Unit VIII and are predominantly filled with carbonates and Fe oxides/hydroxides, chlorites, zeolites, and silica, as well as sediment (Neptunian dikes). Veins usually show a sharp contact with the surrounding host basalt and are either polycrystalline or massive. Claystone is a ubiquitous phase in many carbonate-rich veins, especially in pillow lava flows, and is usually found as very fine aggregates within carbonate veins or as centimeter-thick veins with no preserved textures or structures. Red to green-red halos usually surround the carbonate veins, which are related to the background alteration of interstitial glass, olivine, and occasionally plagioclase and clinopyroxene. Alteration of these basalts remains slight overall, as evidenced by the minimal alteration of interstitial glass as well as the good preservation of plagioclase. Alteration intensity, however, does increase downhole.

### Structural geology

Tilted sedimentary bedding and deformation structures were observed in all lithostratigraphic units. Faults, tilted beds, folds, and mud-clasts observed in Units I, II, and III are likely related to gravity-controlled deposition (e.g., debris flows, slumps, slides, etc.). Unit IV has low recovery and exhibits only a few tilted beds and compaction faults. A total of 47 centimeter-scale faults were measured in the claystone of Units V, VI, and VII. Many of these faults have slickensides and are likely related to clay compaction during lithification. Open fractures and veins are identified in the sparsely to highly plagioclase phyric basalts of Unit VIII. There are no preferred orientations of these structures. Most of the veins are filled by carbonate minerals, Fe oxides, sediment, and secondary minerals. Veins are often haloed by Fe oxide alteration. Vein connectivity is variable; single veins, branched veins, and vein networks are observed. There is no mineral-preferred orientation. Although the seismic profile across Site U1500 shows dipping reflectors in the basalt, we do not observe any clear paleohorizontal or dipping features within these lavas.

## Biostratigraphy

All core catcher samples were analyzed for calcareous nanno-fossil and foraminifer content. Additional samples were taken from the split-core sections when necessary to refine the ages between core catcher samples. Preservation of microfossils varies from poor to good. Overgrown as well as abundant broken fragments are common in the sediment sequences. The total abundance varies from barren to abundant, and most samples exhibit some degree of reworking.

Although recovery is low and ~50% of the samples are barren, the succession is apparently continuous and is tentatively assigned to Miocene–late Oligocene age. The late/middle Miocene boundary (11.6 Ma) can be placed between Samples 367-U1500B-37R-1, 40–41 cm, and 44R-CC. Both calcareous nannofossils and planktonic foraminifers indicate an early Miocene to late Oligocene succession from Cores 367-U1500B-46R through 56R. In the calcareous sandstone just above the basalt (Section 367-U1500B-56R-1), some younger species, such as *Praeorbulina circularis, Globigerinoides subquadratus*, and *Orbulina suturalis* (middle Miocene), are found together with early Miocene to late Oligocene typical planktonic foraminiferal species (*Catapsydrax dissimilis* and *Paragloborotalia opima*). In the same sample, the nannofossil content is represented by long-range species and cannot give a precise age for Core 56R. However, two samples from the veins and intrapillow fill of the basalts in Unit VIII contain poorly preserved calcareous nannofossils and indicate an Oligocene age. The resolution of the age discrepancy in Core 56R requires further postcruise studies.

## Geochemistry

At Site U1500, measurements of organic and inorganic carbon and nitrogen were conducted on one sample per sedimentary core that had relative high recovery, and headspace gas measurements were taken for all sediment cores. In addition, four basalt samples were analyzed for concentrations of major elements and several trace elements using inductively coupled plasma–atomic emission spectroscopy (ICP-AES). Headspace gas values do not exceed 15 ppmv and are mostly below the quantification limit. Carbonate contents are dominated by biogenic carbonate and vary between <1 and 40 wt%, with higher values corresponding to the calcareous-rich lithostratigraphic units. TOC and TOC/TN are low, averaging 0.14 wt% and 4.6, respectively. ICP-AES analyses of basalts from Site U1500 indicate subalkaline mid-ocean-ridge basalt (MORB)-like compositions.

## Paleomagnetism

We conducted AF demagnetization of archive-half sections and AF and thermal demagnetization of representative discrete samples. For the sedimentary samples, AF demagnetization effectively removed the drilling-induced overprint and provided inclinations. Inclination data from the sedimentary long core and discrete samples are in agreement, but because of discontinuous coring and poor recovery in many cored intervals we are not able to correlate these to the standard geomagnetic polarity timescale. The pass-through measurements of the basalts show effective removal of a low-coercivity component; however, it is not clear that we have revealed the ChRM. The basalts sometimes show both positive and negative inclinations upon stepwise AF treatments within a single igneous subunit. The basalts show a more complex pattern when progressive thermal demagnetization measurements are made on discrete samples. The close association of negative inclinations, changes in magnetic susceptibility, and demagnetization behavior with fractures in the cores points to the possibility of a secondary chemical remanent magnetization (CRM) as the source of the reversed intervals in the basalt.

## Petrophysics

We conducted measurements of GRA bulk density, magnetic susceptibility, and NGR on whole-round cores and additional measurements on split cores and discrete samples, including thermal conductivity; PWC *P*-wave velocity; porosity; and bulk, dry, and grain density. In general, bulk densities, *P*-wave velocities, and thermal conductivities increase with depth, whereas porosities decrease with depth as a result of compaction and lithification. However, some properties, such as NGR or magnetic susceptibility, show local variations related to the specific lithology. A significant increase in carbonate content in Subunit VB (1272–1311 m) causes a general decrease in NGR counts and only a slight decrease in the magnetic susceptibility values. Physical properties change significantly in the basalts of Unit VIII (1379–1529 m). Magnetic susceptibility values are two orders of magnitude higher than in the sediment above and vary depending on the degree of alteration. *P*-wave velocity values are also much higher, ranging between 4430 and 5710 m/s, whereas porosity and NGR values are very low compared to the sediment above.

## Correlation to seismic data

We used physical property measurements on cores and samples to correlate Site U1500 data with the available seismic reflection profile. We also used the Site U1500 density and PWC velocity data to create synthetic seismograms that provided additional constraints on the correlation. The TDR obtained for Site U1500 shows substantial agreement with that for Site U1499 as well as Sites U1431 and U1433; in contrast, the Site 1148 TDR exhibits higher velocities in the deeper layers. The comparison between the seismic reflectors and the variations in physical properties and lithology characteristics using the computed Site U1500 TDR shows a good correlation between the high-amplitude seismic reflector at ~6.4 s two-way traveltime (TWT) and the top of basalts of Unit VIII.

## Downhole measurements

Three downhole logging tool strings were run in Hole U1500B; a modified triple combo (sonic velocity, NGR, bulk density, resistivity, and caliper), the FMS-sonic (FMS resistivity images and caliper and NGR), and the VSI (check shot and NGR). During the first run, the tool string encountered an obstruction at 4946 m wireline depth below rig floor (WRF; ~1133 m), and we were unsuccessful in getting the tool string to pass below this depth. We collected FMS data from ~1044 m uphole to the bottom of the casing (842 m). Although the hole had many zones that were significantly enlarged, initial observations of the real-time FMS data indicate that some intervals exhibit relatively good caliper contact and should provide useful resistivity images. A seismic check shot survey with the VSI was able to successfully collect data at one depth in the open hole as well as at the base of the casing. Because this was the last operation conducted during Expedition 367 and we only had a 1 day transit to Hong Kong, data processing and full evaluation of the log data will be conducted after Expedition 367.

# Preliminary scientific assessment

Our assessment of meeting the objectives thus far, at the end of Expedition 367 (halfway through the overall South China Sea Rifted Margin two-expedition program) is as follows.

1. *To determine the nature of the basement within critical crustal units across the COT of the SCS rifted margin in order to discriminate between different competing models of breakup at magma-poor rifted margins. Specifically, to determine if the subcontinental lithospheric mantle was exhumed during plate rupture.*

We have partially completed this objective.

We successfully obtained a very valuable, well-recovered, and unique section of basalt from the base of Site U1500. RCB coring in Hole U1500B penetrated 149.90 m of basaltic rocks (1379.10–1529.00 m) and recovered 114.92 m (77%). Onboard preliminary ICP element analyses done on four samples indicate that they are tholeiitic basalt, compositionally comparable to samples of MORB that were cored during previous Expedition 349 close to the fossil ridge. The basalt may represent a unique lava sequence that erupted in a transitional or earliest seafloor spreading stage (embryonic ocean regime).

Postcruise studies of the Site U1500 basalt should yield compositional information to show if the basalt flows are typical MORB or embryonic oceanic crust and age information to show whether they are rift related or post–seafloor spreading. We can also evaluate if there has been any contamination or mixing with crust or lavas of a different composition.

Coring at Site U1499, on Ridge A, did not reach the crystalline basement. The deepest samples recovered there were pebble- and cobble-sized clasts, inferred to be part of a poorly lithified succession of gravel whose matrix was only rarely preserved in the drilled cores. The sediment that composes many of the cobbles from the gravel unit typically includes mineral and lithic fragments that likely underwent multiple sedimentary cycles. The gravel may have been deposited in a pre- or synrift setting. However, because no underlying crystalline basement was recovered, and biostratigraphic data are sparse, we cannot currently constrain the deposition age of the gravel within the context of basin evolution. Nevertheless, the transition from the gravel to chalk represents a fundamental change in the sedimentary depositional environment. The postcruise determination of age and depositional setting of the cores from Site U1499, including the gravel, will be pivotal to completing Objective 1.

2. *To determine the time lag between plate rupture and asthenospheric upwelling that allowed decompression melting to generate igneous ocean crust.*

We have partially completed this objective.

The tholeiitic basalt from Site U1500 and the overlying sediment will be dated. Nannofossils in the intrapillow fill of the basalts indicate an Oligocene age, implying that the basalt did not erupt before the Oligocene. This information will be refined by postcruise geochronology on the basalt and overlying sediment from both sites using a combination of dating methods (e.g., argon geochronology, detrital zircon geochronology, and detrital low-temperature thermochronologic dating). These results, combined with similar techniques used on the cores obtained by Expedition 368 in basement and sediment at other COT and/or Ridge C sites, will allow us to establish the relative timing of depositional and structural events. This relative timing can be compared to the timing of seafloor spreading in nearby ocean basins to constrain scenarios for the tectonic development of the SCS on both local and regional scales.

3. *To constrain the rate of extension and vertical crustal movements.*

This objective is on track to be completed by postcruise research using the samples we collected and those of Expedition 368, as well as integrating with existing seismic reflection data.

For example, at Site U1500, tilting and faulting have affected the basement reflector (top of the basalts) and overlying sedimentary units. Additional postcruise study on volcanic fabric, fault history, and paleomagnetics as well as ages of the overlying growth-faulted sediment are needed to calculate the net amount and timing of extension and subsidence that is recorded in the seismic reflection data. Similar calculations will be done for other sites. Drilling the sedimentary sequences at Site U1499 will provide another set of information on rifting and breakup history through the postrifting stage. Using a combination of age, porosity, lithology, density, and biostratigraphy, we could calculate the extension rate and vertical subsidence rate. Through cooling history analysis of the basement at Site U1499, we can constrain more about the vertical crustal movements.

4. *To improve the understanding of the Cenozoic regional tectonic and environmental development of the Southeast Asia margin and SCS by combining Expedition 367/368 results with existing ODP/IODP sediment records and regional seismic data.*

This objective is partially completed, but we already have made major progress and have obtained important results.

The postrift sediment cored during Expedition 367 provided two major contributions to our understanding of the late Cenozoic tectonic and environmental history of the northern margin of the SCS. The first contribution involves new time-depth constraints on some of the major seismic reflectors that are mapped regionally throughout the basin. This was done by integrating micropaleontology ages, petrophysics, and borehole logging data with the existing seismic reflection data. The second contribution involves improvements to the lithostratigraphic record of the Miocene and younger sediment. Two critical sedimentary successions were observed at both sites: an upper succession of hemipelagic and turbidite deposits and a lower succession of red claystone and chalk that was recovered near the bottom of each site. The upper succession likely records processes that delivered sediment from the shallow shelf of the northern SCS to the deeper parts of the basin. The abnormally high sedimentation rates, especially at Site U1500 (12–27 cm/ky for the upper Miocene sequence), indicate strong erosion from source areas and efficient transport. The lower succession of red clay and chalk may correlate to a basin-wide event related to deep circulation of oxygenated water from the western Pacific, prior to the closure of the Luzon Strait in the middle Miocene. Postcruise research on the red clay will combine with observations of similar pelagic sediment recovered in the central basin during Expedition 349 to constrain the environmental and tectonic evolution of the Southeast Asia margin.

Postcruise research using samples from Expedition 367 will continue to improve on these contributions to Objective 4. This research should be channeled into three general avenues:

1. Correlation of the chronostratigraphic record among Sites U1499, U1500, the sites that will be drilled during Expedition 368, and previous IODP and ODP expeditions in the SCS;

2. Provide new data (e.g., detrital zircon geochronology) to constrain the sedimentary provenance of the Miocene hemipelagite and turbidite deposits; and

3. Reconstruct paleoceanographic conditions favorable to pelagic red clay deposition through geochemical and geophysical techniques.

A complete set of observations relative to Objective 4 will use the results of Expeditions 367 and 368 together with seismic stratigraphic correlations to improve our understanding of the regional tectonic and environmental development.

# Operations

The South China Sea Rifted Margin program was implemented with operations scheduled at four sites during Expeditions 367 and 368. During Expedition 367, we cored and logged at Sites U1499 and U1500. The primary drilling operations during this expedition are summarized in this section and in Table **T1** and Figures **F6**, **F9**, and **F10**.

At Site U1499, we conducted operations in two holes. We cored with the APC/XCB systems in Hole U1499A from the seafloor to 659.2 m and recovered 417.05 m (63%). We installed casing in Hole U1499B to 651 m; cored with the RCB from 655.0 to 1081.8 m, recovering 150.64 m (35%); and then conducted two wireline logging runs below the casing downhole to ~65 m above the base of the hole.

At Site U1500, we conducted operations in two holes with the primary objective of sampling and logging the lowermost sediment and underlying basalt. We successfully penetrated from the seafloor to the sediment/basalt contact at 1379 m and 150 m into the underlying basalt. The sedimentary section was not continuously cored, and recovery in the cored intervals was highly variable and rather poor (30%). In contrast, core recovery in the basalt was excellent (77%). We collected log data in Hole U1500B from 842 m (base of casing) to a total depth of 1133 m.

We knew we would have to install casing to achieve the deep objectives at Site U1500. Our operations in Hole U1500A were designed to provide information on formation characteristics and drilling conditions so that we could decide the length of casing to drill into the seafloor at the second, deep-penetration Hole U1500B. Given this purpose and the amount of time to drill the second, deep hole, we did not core continuously in Hole U1500A. In Hole U1500A, we

- Drilled without coring from the seafloor to 378.2 m,
- Cored with the RCB from 378.2 to 494.6 m and recovered 26.5 m (23%),
- Drilled without coring from 494.6 to 641.2 m, and
- Cored with the RCB from 641.2 to 854.6 m and recovered 67.2 m (31%).

In Hole U1500B, we

- Drilled a reentry funnel and 842 m of 10.75 inch casing into the seafloor,
- Continuously cored the sediment sequence with the RCB from 846.0 to 1379.1 m (533.1 m cored; 164.7 m recovered; 31%),
- Continuously cored with the RCB 150 m into the underlying basalt from 1379.1 to 1529.0 m (114.92 m recovered; 77%), and
- Collected downhole log data with three tool string logging runs from 842 m (base of casing) to a total depth of 1133 m (~400 m above the base of the hole).

## Hong Kong port call

The South China Sea Rifted Margin Expedition 367 started at 0812 h (all times are UTC + 8 h) on 7 February 2017 with the first line ashore at the China Merchants Wharf in Hong Kong. The Co-Chief Scientists and IODP staff moved onto the ship and started crossover with their Expedition 366 counterparts. Initial loading of incoming shipments began. The Expedition 367 scientists boarded the ship in the morning of 8 February, got settled in their rooms, were introduced to life on board the *JOIDES Resolution*, and participated in an initial laboratory and ship safety tour. The scientists were then introduced to the information technology on board the ship, started to connect their computers to the shipboard network, and half of the science party went on a core-flow tour. Transfer of incoming and outgoing shipments continued throughout the day. Arriving sea freight was partially loaded, along with fresh and refrigerated food products and 300 metric tons of potable water. All departing freight was moved to the pier. On 9 February, the day began with introductions of the Expedition 367 scientists and JOIDES Resolution Science Operator (JRSO) shipboard staff followed by a presentation of the expedition scientific objectives by the Co-Chief Scientists. The rest of the day's science meetings had to be postponed until the next day so that seven scientists could address issues with their travel documents. Major port call activities on 9 February included loading of 40 short tons of drilling mud, 987.3 metric tons of marine gas oil, sea freight, and frozen food as well as offloading of frozen shipments from the previous expedition. Because of a missed boat transfer in Shanghai, China, a shipment of essential hardware (reentry cones, casing, and mud motors) was delayed until 10 February. Because of the time required to load this essential hardware, our departure was delayed by 1 day to 13 February.

On 10 February, scientists were introduced to shipboard deliverables, met in lab groups with their JRSO technical staff team members, underwent the Captain's introduction and safety orientation, and the other half of the science party went on a core-flow tour. A Texas A&M University System film crew spent the day filming some promotional videos and were escorted around the ship. In addition to routine loading/offloading, the trucks with our delayed shipment of essential hardware started arriving in the late afternoon of 10 February. After carefully calculating the remaining work, arrangements were made with the agent and immigration authorities for a departure at 1200 h on 13 February.

On 11 February, the scientists were introduced to drilling/coring/logging operations, our shipboard Educator and Journalist gave an overview of their plans for the expedition, and the Captain held the first fire and boat safety drill. In the afternoon, the scientists shared their individual research interests for the expedition with each other. Loading of the essential hardware continued throughout the day, and by the end of the day all casing had been secured in the riser hold. All that remained of port call activities was to load five flats of drill pipe and final securing of cargo prior to departure.

We finished loading all remaining operations hardware on 12 February, including 288 joints of drill pipe. We also spooled new coring line onto the forward coring winch, offloaded trash prior to sailing, secured all equipment for heading out to sea, and made necessary arrangements with port authorities for departing the next day.

At 1000 h, 13 February, immigration authorities boarded the ship and the vessel was cleared for departure. The harbor pilot arrived on board just before noon, and the vessel was under way with

the last line released at 1215 h on 13 February. We proceeded to the pilot station, and after a 7 nmi transit the pilot disembarked at 1248 h. Our 277 nmi transit to Site U1499 took 28.0 h with an average speed of 9.8 kt.

## Site U1499

### Hole U1499A

After arriving at Site U1499 at 1615 h on 14 February 2017, we lowered the thrusters, deployed a seafloor beacon, assembled two extra stands for RCB coring later in the expedition, put together the APC/XCB bottom-hole assembly (BHA), and lowered it to 3749.4 m below rig floor (mbrf) in preparation for coring. As each piece of the drill string was assembled, its length was measured and its interior was verified to be unobstructed. The top drive was picked up, the entire string spaced out to place in preparation for starting coring, and a wiper pig was pumped through the drill string to clean rust and debris from the inside of the drill string. The calculated precision depth recorder (PDR) depth for the seafloor at Hole U1499A was 3774.4 mbrf; we chose to place the bit at 3769 mbrf to take the first core. An APC core barrel was lowered to the bit, and coring in Hole U1499A started at 0930 h on 15 February. Based on a mudline core recovery of 7.5 m, we calculated the seafloor to be at 3771.0 mbrf (3760.2 m below sea level [mbsl]). APC Cores 367-U1499A-1H through 18H penetrated to 162.4 m and recovered 167.51 m (103%). All APC cores used nonmagnetic core barrels and were oriented. Formation temperature measurements (APCT-3) were made while taking Cores 4H, 6H, 8H, 10H, 12H, and 14H.

APC Cores 12H through 18H (102.5–162.4 m) encountered increasingly firm formation, and the core barrel did not fully penetrate the formation for many of them. Because of our primary expedition objectives, we switched to XCB coring instead of first using the half-length APC (HLAPC) system, which would take twice as long to penetrate the formation.

XCB Cores 19X through 57X penetrated from 162.4 to 540.7 m and recovered 227.37 m (60%). XCB core recovery was highly bimodal. We had quite high core recovery in the fine-grained intervals (Cores 19X through 36X from 162.4 to 337.0 m with 158.99 m recovered [91%] and Cores 44X through 50X from 404.9 to 472.8 m with 65.19 m recovered [96%]). We had very fast penetration rates and extremely low recovery in unconsolidated sands (Cores 37X through 43X from 337.0 to 404.9 m with 1.37 m recovered [2%] and Cores 51X through 57X from 472.8 to 540.7 m with 1.82 m recovered [3%]). One exception was Core 25X, which came back with only 2 cm of core, but the core liner appeared to have had sediment in it, so we inferred that the sediment was fine grained, and that it fell out of the core barrel while this was being retrieved.

Once we encountered the unconsolidated sands, we started circulating mud sweeps (30 bbl at 337.0, 346.7, 375.8, 404.9, 443.7, 472.8, 492.2, 511.6, and 531.0 m). While making a connection at 492.2 m, the drill string became stuck and could not be rotated. We circulated an additional 50 bbl of mud, were able to regain rotation, and resumed XCB coring in Hole U1499A. Cores 58X through 67X penetrated from 540.7 to 637.7 m (20.37 m recovered; 21%). For the first eight cores (58X through 65X), the bit penetrated very quickly through 77.6 m and recovered only 4.16 m (5%), so we inferred that the sediment is predominantly unconsolidated sand. Core 66X had slower penetration and 100% recovery in the finer grained formation. However, the penetration rate increased again in Core 67X, indicating that we encountered sand again. The last core on 19 February (Core 68X) also cut very quickly and had almost arrived back on the rig floor (~100 mbrf) when the low-clutch diaphragm

in the drawworks failed at 2245 h on 19 February; we could not raise the drill string. We secured the drill string and circulated, rotated, and pumped a mud sweep every hour to keep the drill string from getting stuck while repairing the ruptured diaphragm. After the 24.5 h it took to repair the drawworks, we were finally able to open the drill string and get Core 68X out of the drill string at 2320 h on 20 February. We had suspected it would be empty because it cored very quickly through inferred sand, but it also had been sitting in the drill string for a full day. Although coring recovery was quite variable, very close to XCB coring refusal, and the finer grained formation we did recover was getting quite hard, we wanted to penetrate a few more cores to verify an appropriate formation to set the base of the casing to be deployed in our next hole (firm formation, not sand).

Cores 69X through 71X penetrated quite slowly from 647.4 to 659.2 m and recovered 1.8 m of hard sedimentary rock; we decided this was an appropriate interval for the base of the casing. The driller then circulated the entire hole with mud to minimize risks of hole problems as we pulled the drill string out of the hole. We started pulling the drill string out of Hole U1499A at 0815 h on 21 February. We kept the top drive installed until the bit was at 299 m, above the uppermost interval of unconsolidated sand. The bit cleared the seafloor at 1230 h on 21 February and arrived on the rig floor at 2015 h, ending Hole U1499A. APC/XCB coring in Hole U1499A penetrated 659.2 m. As mentioned above, core recovery was highly variable (formation dependent), and core recovery was a total of 417.05 m (63%). We suspect that unconsolidated sand accounted for the poor recovery. The overall drilling, coring, and formation information from Hole U1499A was used for planning the casing installation for the second hole to achieve our deep-coring and logging objectives.

### Hole U1499B

We offset the ship 20 m east of Hole U1499A and conducted required routine rig servicing (drill line slip and cut). At 2345 h on 21 February, we started preparing the rig floor for assembling the reentry cone and 651 m long casing to be drilled into the seafloor in Hole U1499B.

We spent all of 22 February and the first part of 23 February assembling the 10.75 inch casing and the drilling string we would use to drill it into the seafloor. This included

- Moving the mud skirt over the moonpool,
- Assembling 651 m of 10.75 inch casing, lowering it through, and latching it into the mud skirt, and
- Assembling a 9.875 inch tricone bit, underreamer set to 12.75 inches, and mud motor and lowering them through the casing hung off in the moonpool.

At 0430 h on 23 February, we finished putting together the final parts of the drilling assembly. This included attaching the upper part of the casing running tool (which contains the hydraulic release tool [HRT]) and attaching the reentry funnel. We started lowering the entire 651 m long casing string and drilling assembly to the seafloor and deployed the camera system at 1115 h on 23 February to monitor the reentry funnel while the casing was being drilled into the seafloor. When the pilot bit that extends 2.71 m below the casing shoe was just above the seafloor, the drillers measured the pressures at various pump rates to get information to compare to those when we start penetrating the formation. Drilling in Hole U1499B started at 1535 h on 23 February. While drilling the casing into the seafloor, we circulated 25 bbl mud sweeps at 152.6, 327.8, 356.98,

493.1, 619.8 m. We continued to drill the casing into the seafloor until the mud skirt landed on the seafloor.

We deployed the go-devil to activate the casing running tool, which released the casing at 2300 h on 24 February. We retrieved the entire drilling assembly, with the bit clearing the seafloor at 0230 h on 25 February, and the bit arrived back on the rig floor at 1230 h on 25 February. After taking apart the drilling assembly and flushing the mud motor, underreamer, and bit with freshwater, we began preparing the rig floor for RCB coring. We started assembling the RCB BHA at 1430 h on 25 February, and the rest of the day was spent lowering it to the seafloor. At 2230 h on 25 February, the subsea camera was deployed. Once the RCB bit and camera reached the seafloor, we started searching for the Hole U1499B reentry funnel at 0215 h on 26 February. After we were unable to find it relatively quickly (as is usual), we initiated an expanding 5 m grid search. After just over 6 h, we eventually found the reentry funnel cone. It was clearly visible inside a small crater of sediment located about half-way (~10 m) back toward and a little south of Hole U1499A to the west. Also, the top of the reentry funnel appeared to be close to level with the top of the cuttings pile. After only 10 min of maneuvering, we reentered Hole U1499B at 0825 h on 26 February, started lowering the RCB bit down through the casing, and recovered the camera system. As the bit was being lowered, it encountered sediment inside the casing at 571 m, 80 m above the casing shoe. This was assumed to be sand which was drawn back into the casing as the drilling stinger assembly (with pilot bit, underreamer, and mud motor) used to drill the casing in was withdrawn from the casing. We picked up the top drive, deployed a core barrel at 1230 h, and washed back to the bottom of the hole at 655 m (4 m below the base of the casing). We circulated 30 bbl of mud, retrieved the core barrel (empty), and at 2230 h on 26 February, we started RCB coring in Hole U1499B.

On 27 February, RCB coring in Hole U1499B penetrated from 655.0 to 790.8 m with an overall recovery of 41.44 m (Cores 367-U1499B-2R through 15R; 31%). However, recovery continued to be highly variable and formation dependent. In fine-grained intervals, we had higher recovery (53%) and steady, relatively slow penetration rates (Cores 2R through 3R from 655.0 to 674.4 m, Cores 9R through 10R from 722.9 to 742.3 m, and Cores 13R through 15R from 752.0 to 790.8 m). In other intervals, inferred to consist of loosely consolidated coarse-grained sand, we had very low recovery (0.7%) and very quick penetration rates. The drillers noted these intervals at 672.9–727.6 and 739.3–759.7 m, which correspond mostly with Cores 4R through 8R (674.4–722.0 m) and 11R (742.3–752.0 m). We circulated 30 bbl mud sweeps at 684.1, 713.2, 742.3, 761.7, and 781.1 m. At first light on 27 February, a boat (M/V *Taikoo*) with critical spares for the drawworks clutch arrived on site, and the transfer was completed.

We continued RCB coring from 790.8 to 897.5 m (Cores 16R through 26R; 72.33 m recovered; 68%) and circulated 30 bbl mud sweeps at 810.2, 839.3, and 878.1 m. Each of these cores (16R through 26R) took from 20 to 60 min to cut. Another fast-drilling zone from 825.0 to 834.0 m was also noted by the drillers. After Core 26R, however, we encountered a substantial formation when Core 27R took over 2 h (205 min) to cut. RCB Cores 27R through 29R continued in very hard formation. These cores took 120–205 min to cut, penetrated 29.1 m from 897.5 to 926.6 m, and recovered 16.43 m (56%). However, Core 30R took only 45 min to cut (as opposed to 205, 130, and 120 min for the cores just above). In addition, when the bit was being raised off bottom to recover the core, the drill string became stuck momentarily, so we circulated 30 bbl of

mud, and hole conditions improved. The penetration time for Core 31R went back up (130 min), but the drill string became temporarily stuck again. This time we circulated 90 bbl of mud, and coring was able to continue.

RCB Cores 31R through 38R penetrated 77.6 m from 936.3 to 1013.9 m and recovered 8.66 m (11%). It took from 2 to >3 h to cut each core. The drill string became stuck momentarily while cutting Core 33R. We circulated 30 bbl of mud after cutting Cores 32R and 35R through 37R.

Because we decided to stop coring to change the RCB bit to core deeper and the bit had accumulated 40.6 rotating hours, we circulated the cuttings out of the hole with 70 bbl of mud after Core 38R. Before pulling the bit up into the casing and out of the hole, we first raised the bit up to 780 m, circulated the hole with 35 bbl of mud, and then filled the uncased (open) part of the hole with 235 bbl of heavy mud (11.0 lb/gal; barite). This was intended to help stabilize the hole while we changed the bit and reduce the amount of fill we might encounter when we reentered the hole to resume RCB coring. This was also expected to give us some indication of the hole conditions we might encounter for planned downhole logging after coring had finished. Because we had some challenges locating the hole the first time we reentered, we lowered the subsea camera system to observe the reentry funnel as we pulled the bit out of the hole. While we were still in the hole, we could see the drill pipe clearly in the center of the crater created by the cuttings mound. Although the reentry funnel's concentric black and white stripes were not visible, we didn't anticipate problems finding and reentering the hole. The bit was pulled out of the hole at 1655 h on 3 March, and we spent the rest of the day recovering the drill string (except for a 0.5 h repair of the pipe racker).

We finished recovering the drill string at 0215 h on 4 March, attached a new RCB bit (C-7), lowered it to the seafloor, and then deployed the subsea camera system at 0915 h. We paused rig floor operations from 0915 to 1045 h to conduct required routine rig servicing (drill line slip and cut) before we resumed lowering the drill bit to the seafloor. At 1345 h on 4 March, the bit and camera were in position, and we were able to immediately see the reentry funnel in the center of the cuttings pile caldera. It took us 22 min to position the bit over the funnel and reenter Hole U1499B at 1407 h on 4 March. We retrieved the camera and lowered the bit down through the 651 m of casing to 848.1 m in the open hole. We installed the top drive and circulated/rotated until 987 m, only ~27 m from the bottom of the hole, before the bit encountered any resistance. This was easily penetrated, and we only encountered 1 m of fill on the bottom of the hole. At the end of the day, we pumped 40 bbl of mud to clear cuttings from the hole and retrieved the core barrel that was in place while getting back to the bottom of the hole. We resumed RCB coring from 1013.9 m at 0115 h on 5 March. Cores 39R through 43R penetrated from 1013.9 to 1062.4 m and recovered 4.1 m (4%). We pumped 30 bbl of mud after each of these cores.

At 0100 h on 6 March, Core 44R arrived on the rig floor (1062.4–1072.1 m; 0.45 m recovered; 5%), and we dropped the next core barrel to start cutting Core 45R. While this core was being cut, there were periods of erratic torque, high pump pressures, and some short times when the drill string could not be rotated. The driller raised and lowered the drill string and was able to keep coring. Just after we put the core line into the drill string to retrieve Core 45R, the pipe became stuck. For ~45 min, we worked the drill string until it was freed at 0615 h on 6 March. We then removed the core line from the drill string. We raised the bit back up to 994 m and worked to clean out the hole. Eventually at 1045 h, conditions

had improved enough that we retrieved Core 45R at 1150 h (1072.1–1081.8 m; 0.09 m recovered; 0.9%). We spent the next 9 h attempting to wash, ream, drill, and circulate our way back to bottom. However, we never were able to get below ~1053 m (~30 m above the bottom of the hole) without the drill string getting stuck. At 2045 h on 6 March, we decided that further attempts to get back to the bottom of the hole and core deeper were not reasonable, so we started to prepare the hole for wireline logging. We circulated 50 bbl of mud to clean cuttings out of the hole, retrieved the core (wash) barrel that was in place during the hole remediation efforts, and lowered the rotary shifting tool on the coring line to release the bit in the hole.

After the bit was released in the bottom of the hole at 0000 h on 7 March, we raised the end of the pipe from 1052.7 to 877.3 m and shifted the mechanical bit release sleeve back into the circulating position. We then raised the end of the pipe to 780 m and pumped 235 bbl of heavy mud into the hole to help maintain good hole conditions for logging. At 1030 h on 7 March, we had raised the end of pipe back inside the casing to 85.1 m and started to prepare the rig floor for logging. Our first logging tool string consisted of the resistivity, velocity, density, and NGR tools. We started lowering it at 1345 h on 7 March. The tool string was able to reach 1020 m, and we successfully logged from that depth up to the base of the casing at 651 m. Log data were also collected up the casing and drill pipe to the seafloor. The tool string arrived back at the rig floor at 2215 h on 7 March. Based on the first logging run results, we decided to conduct a second logging run with the FMS and NGR tools.

We assembled the FMS and NGR tools and started lowering them at 0130 h on 8 March. The tool string was able to reach 1010 m and we were able to make two passes of the open hole up to the base of the casing at 651 m. Initial results showed that we collected some excellent data in intervals with good borehole diameter. The tool string arrived back on the rig floor at 0925 h, and all of the logging equipment was off the rig floor at 1030 h on 8 March. We pulled the end of the drill string out of Hole U1499B at 1120 h, recovered the seafloor beacon, and started the transit to Site U1500 in dynamic positioning mode just before 1300 h on 8 March. While in transit, we continued to recover the drill string (arrived back on the rig floor at 1830 h on 8 March) as well as assembled a new RCB bit and started lowering it to the seafloor. We spent a total of 22.1 days at Site U1499.

## Site U1500

### Hole U1500A

At 0415 h on 9 March 2017, we deployed the subsea camera system and observed the bit tag the seafloor to establish the water depth (3801.7 mbsl). After recovering the camera system, we started drilling without coring in Hole U1500A at 0935 h on 9 March. Unfortunately, at 1930 h with the bit at 340.5 m, the drawworks clutch diaphragm that had been replaced earlier in the expedition failed. The clutch diaphragm was repaired with one of the new diaphragms that had been delivered to the ship by boat on 27 February. As soon as it was fixed (0930 h on 10 March), we resumed drilling without coring from 340.5 to 378.2 m. While drilling down, we pumped 30 bbl mud sweeps at 350.2 and 378.2 m. We recovered the center bit and started RCB coring at 1245 h on 10 March. Cores 367-U1500A-2R through 13R penetrated from 378.2 to 494.6 m and recovered 26.5 m (23%). We drilled without coring from 494.6 to 641.2 m and then resumed RCB coring to the total depth of 854.6 m.

Except for a few short intervals (Cores 2R through 4R from 378.2 to 407.3 m, Cores 24R through 27R from 728.5 to 767.3 m, and

Cores 35R through 36R from 835.2 to 844.9 m), core recovery was quite poor. In contrast, the cores that took 15 min or more to cut had better recovery (from 0.88 to 8.93 m; average recovery = 59%). We pumped frequent mud sweeps through the entire cored interval.

A formation change occurred at 728.5 m with Cores 24R through 27R (728.5–767.3 m), taking 30–50 min to cut with substantially improved recovery (32.1 m; 83%) of clay/claystone. We thought this would be a good formation for the base of our planned Hole U1500B casing until Core 28R once again reentered a fast-penetrating, low-recovery interval inferred to be sand. Following this, Cores 29R through 36R penetrated from 770.0 to 854.6 m and recovered 27.6 m (36%). The majority of the core recovered was in Cores 30R, 33R, 35R, and 36R (25.29 m). For the other cores, penetration rates were, once again, very fast and recovery very low (2%–9%; inferred to be less consolidated silt/sand). When the last two cores (35R and 36R) encountered stable, well-consolidated formation, we decided we had met our primary objective of determining formation conditions at Site U1500 and an appropriate casing set point for our next hole at this site. So, we pulled the bit out of the hole, and it cleared the seafloor at 2330 h on 13 March. Based on the Hole U1500A information (cores, drilling, and borehole conditions), we decided that to achieve our deep-coring and logging objectives at this site, we would drill 842 m of casing into the seafloor at Hole U1500B. This placed the base of the casing in the relatively fine grained stable formation recovered in the last two cores and would isolate the multiple intervals of unstable formation above (inferred sand/silt). After the bit arrived back on the rig floor at 0640 h on 14 March, we disassembled the bit, cleared the rig floor, and conducted required routine rig servicing (drill line slip and cut).

### Hole U1500B

From 0900 on 14 March to 0400 h on 15 March we prepared the casing running tool (HRT), assembled 842 m of 10.5 inch casing, and latched it into the mud skirt sitting on the moonpool doors. We then assembled and tested a 846 m long drilling assembly composed of a 9.875 inch tricone bit, underreamer (set to 12.75 inches), and mud motor. This drilling assembly was lowered through the casing, the HRT attached to the top of it, and then secured to the mud skirt/casing. At 1130 h on 15 March, the entire system was lowered through the moonpool and then to the seafloor. We deployed the subsea camera system at 2015 h on 15 March and installed the top drive shortly thereafter (2315 h).

At 0035 h on 16 March, we started drilling the casing into the seafloor at Hole U1500B. Along the way, we circulated 30 bbl of mud at multiple depths (335.6, 374.6, 394.0, 423.1, 452.2, 481.4, 510.6, 539.6, 568.8, 597, 627, 656, 685, 714, 744, 774, 802, and 832 m). Drilling the casing into the seafloor proceeded smoothly until ~779 m (0800 h on 17 March) when we observed the mud skirt and reentry funnel rotate very quickly indicating that torque had built up in the drill string and then suddenly released. At the same time, we also observed that the penetration rate slowed down substantially. We suspected that one or more of the underreamer arms had lost its cutting structure (roller cone). Our options at this point were limited. We could continue to drill the bit in to the full depth or pull it back to the ship, shorten the casing string, and try to drill that in. We had only ~63 m more of penetration until the casing was fully installed. Based on the coring information from Hole U1500A, much of this interval was expected to be loosely consolidated fast-penetration formation with only a couple of short intervals of firm formation. So, we continued to drill in. Although penetration rates slowed quite a bit, we were able to continue advancing the entire

system until a reduction in drill string weight indicated that the mud skirt had landed on the seafloor at 1740 h on 17 March (Figure **F10**). This fact led us to suspect that if the underreamer cutters had come off, they likely had been pushed off into the borehole wall behind the casing. We dropped the go-devil to activate the HRT, and the drilling assembly released from the casing at ~1833 h on 17 March. We raised the bit and underreamer back up to 841.4 m, inside the casing, and filled the annulus between the casing and the drill pipe with 100 bbl of mud to inhibit sand from being sucked back up into the casing as we pulled the drilling assembly out of the hole (as previously happened at Hole U1499B). We then pulled the drill string out of the hole. After the bit cleared the seafloor (2220 h on 17 March), we conducted a short survey of the reentry system, which was barely visible in the cutting mound.

Once we finished recovering the drilling assembly and the underreamer arrived back on the rig floor (0730 h on 18 March), we observed that all of its cutting structures were still attached. However, one of them was clearly damaged (failed bearing assembly) and likely the cause of the torque event and subsequent reduction in penetration rate. We started assembling the RCB BHA at 0915 h on 18 March and lowered it to the seafloor. We deployed the subsea camera system at 1615 h, started searching for the Hole U1500B reentry funnel, and after only 6 min of maneuvering we reentered Hole U1500B at 1845 h on 18 March. We recovered the camera system, lowered the bit through the casing, and installed the top drive in preparation for RCB coring. We lowered the bit into the open hole below the end of the casing (842 m), found only 1 m of fill, circulated 25 bbl of mud displacing the heavy mud out of the hole, and started RCB coring at 0115 h on 19 March. The uppermost 5.3 m of the first core taken after installing the casing (Core 2R) was composed primarily of heavy mud mixed with some cuttings.

Overall core recovery in Hole U1500B was very poor over a significant interval of the sedimentary section, particularly from 893.8 to 1233.3 m (lithostratigraphic Unit IV). Cores from this interval (Cores 7R through 41R) penetrated 339.5 m and recovered only 51.3 m (15%). For cores in this interval that cut quickly (≤15 min), core recovery was only 7%, and we inferred the formation is likely dominated by unconsolidated sand/silt. In contrast, recovery in cores that took longer to penetrate (20–55 min) was higher (41%) and recovered sandstone with claystone and siltstone interbeds.

While cutting Core 42R, we encountered a substantial formation change at 1235 m, and core recovery increased to 66% for Cores 42R through 45R. The time to cut Cores 43R through 45R also increased to 40–80 min. The formation change is also reflected in the recovered cores that are dusky red claystones with greenish alteration zones as well as a few interbedded sandstone layers. Cores 46R through 50R penetrated from 1272.1 to 1320.6 m and recovered 30.2 m (62%). Although it took quite a long time to cut each of these cores (1.8–3.8 h), the penetration rate was very smooth and hole conditions were quite good. Cores 51R through 57R then penetrated from 1320.6 to 1388.5 m and recovered 32.4 m (48%). After Core 51R took 100 min to cut, the next five cores (52R through 56R) penetrated quite quickly; all but one took only 5–25 min, and had relatively lower recovery (31%). Core 57R cut slowly (3.6 h) but smoothly and consistently and recovered 8.34 m that is almost entirely basalt. Cores 58R through 60R continued in basalt penetrating from 1388.5 to 1415.9 m and recovering 19.9 m (73%). These cores also cut slowly (4.3–5.4 h) but mostly smoothly and consistently. Because we had 52 rotating hours on the bit and we wanted to core and log deeper in Hole U1500B, we decided to retrieve the drill string to change the RCB bit. We circulated cuttings out of the hole, raised the bit up to 1242 m and pumped 235 bbl of weighted (11.0 lb/gal) mud into the hole to stabilize it while we changed the bit. We then pulled the drill string out of the hole (removing the top drive at 1066.0 m), and the bit cleared the seafloor at 2340 h on 25 March.

Before we recovered the drill string, we paused operations for 2 h to conduct routine rig servicing (drill line slip and cut). The bit arrived on the rig floor in good shape at 0845 h on 26 March. We attached a new RCB bit for basement coring (C-7) and lowered it toward the seafloor. Once the bit was at the seafloor along with the camera system, we started searching for the reentry funnel at 1730 h on 26 March. After a short search, we saw streaks of cuttings on the outside of the mound of drill cuttings around the hole. We moved the bit over the clearly visible reentry funnel and reentered Hole U1500B at 1755 h. We lowered the bit through the casing and into the open hole below. As we were doing this we had the float valve shifted into the open position, which allows water to easily pass through the bit. If it's in the closed position we have to stop periodically to fill the drill string with water as we lower it. As we lowered the bit, it encountered a bridge at ~1067 m, and sediment appeared to block flow through the bit. We then pulled up a little bit and deployed a core barrel to try to clear the obstruction in the bit and to close the float valve so we could wash/drill back down the hole to resume RCB coring.

The core barrel that we dropped to clear the obstruction in the bit did not land properly at the bottom of the drill string. We deployed the core line to retrieve the core barrel and found that it had landed ~42 m above the bottom of the drill string. We made three unsuccessful attempts to pull the core barrel back out. We then raised the bit from 1018 to 454 m inside the casing (above the top of the weighted mud) and still could not free the core barrel and reestablish circulation. We made two more unsuccessful attempts with the bit at 249 m and then above the seafloor. At 1530 h on 27 March, we decided the only way to fix this problem was to retrieve the entire drill string. At 0000 on 28 March the bit had reached 58 m below the rig floor, and we spent most of the early morning of 28 March recovering the final parts of BHA on the rig floor and cleaning out sediment (cuttings, sand, etc.) that filled the lowermost ~40 m of it. The sediment had worked its way above the core barrel. At 0700 h on 28 March, we started reassembling the RCB BHA and lowering it to the seafloor. We deployed the camera system, dropped a core barrel to close the float valve, and started to position the bit over the reentry funnel at 1830 h on 28 March. We reentered Hole U1500B at 1930 h, recovered the camera system, and lowered the bit down to 804.3 m in the casing. At 2315 h on 28 March, we started to install the top drive in preparation for lowering the bit through the base of the casing (842 m) and into the open hole below. However, at 0045 h on 29 March we discovered a problem with the top drive (one of the counter-balance cylinders). After fixing it, at 0400 h on 29 March we resumed lowering the bit. After exiting the base of the casing and down into the open hole, the bit started encountering some resistance at ~1066 m. We washed from there back down to the bottom of the hole at 1415.9 m, pumping 30 bbl of mud at 1008, 1115, 1203, 1232.4, and 1300.52 m. At the bottom of the hole, we pumped 35 bbl of weighted (11.0 lb/gal) mud to clean the cuttings out of this deep hole. We planned to continue using weighted mud in Hole U1500B as we penetrated deeper. We recovered the core barrel that was in place while getting the bit back to bottom (ghost Core 61G; 2.36 m recovered), deployed a fresh core barrel at 1745 h on 29 March, and resumed RCB coring. Core 62R

arrived on the rig floor at 2230 h on 29 March after penetrating 2.5 m (1415.9–1418.4 m) and recovering 2.36 m (94%). This shorter penetration was necessary to adjust pipe connections at the rig floor.

Although Core 63R recovered 3.6 m of very nice basalt, it took much longer to cut (8 h) and the core pieces had become stuck inside the plastic core liner and in the core catcher sub. It is likely that the recovered material came from the upper part of the cored interval, then jammed, and the rest of the core got ground up, washed away, and never entered the core barrel. This may have also contributed to the slow penetration rate (at least after the core jammed off). So, we decided to cut only half-length cores. Cores 64R through 73R then penetrated from 1428.0 to 1475.9 m and recovered 40.0 m (84%). Although the cores took from 2.3 to 4.7 h to cut, the recovery and core quality of the basalts was excellent.

Because the bit had accumulated 44 h of rotating time, hole conditions remained good, and we planned to continue to core deeper into basement and collect downhole logs, we decided to stop coring to change the bit. After cutting Core 73R, we circulated cuttings out of the hole with two 35 bbl weighted mud sweeps and raised the bit to 1387.8 m where we removed the top drive. We then raised the bit to 1242.1 m and filled the hole with 235 bbl of weighted mud to stabilize it while we changed the bit. Once the mud was in place, we raised the bit to just below the seafloor (45.7 m) and deployed a secondary reentry (free-fall) funnel on top of the first one that we previously drilled into the seafloor with the casing (Figure **F10**). This secondary reentry funnel was intended to block the large pile of cuttings around the hole from falling back in while we continued our Hole U1500B operations. After the funnel was dropped at 2208 h on 1 April, we continued to circulate to minimize the amount of cuttings in the seafloor structure while the secondary funnel landed. We deployed the subsea camera system at 2330 h on 1 April so that we could observe the bit being withdrawn from Hole U1500B.

At 0100 h on 2 April, we observed the bit being pulled out of the hole with the subsea camera system and then recovered the drill string with the bit arriving back on the rig floor at 0840 h. We installed a new bit more appropriate for hard formations (C-9), lowered it to the seafloor, and started positioning the ship to reenter Hole U1500B at 2000 h on 2 April. We reentered the hole at 2100 h, recovered the camera system, and lowered the bit down through the casing.

Before lowering the new RCB bit into the open hole below the casing, we paused for 2 h to conduct routine rig servicing (drill line slip and cut, lubricate the rig). Once in the open hole, the bit encountered some resistance (bridge/ledge) at ~947 m and we reamed from there to ~950 m. The bit passed quite easily from there to the bottom of the hole where ~0.5 m of hard fill was drilled out. After circulating two 35 bbl mud sweeps, we recovered the core barrel that was in place while getting back to the bottom of the hole. We resumed RCB coring from 1475.9 m at 1730 h on 3 April. Cores 74R through 83R penetrated from 1475.9 to 1529.0 m and recovered 39.8 m (75%).

The last core of Expedition 367 (Core 83R) arrived on the rig floor at 1530 h on 5 April. We stopped coring so that we would have time to collect downhole log data with three different tool strings (triple combo, FMS-sonic, and VSI). In preparation for logging, we circulated cuttings out of the hole (two 35 bbl mud sweeps) and raised the bit to 1416 m where we removed the top drive. We then continued to raise the bit to 1242 m and spent 1 h (1730–1830 h on 5 April) filling the borehole (and well up into the casing) with 300

bbl of weighted (11.0 lb/gal) mud to increase our chances the hole would stay open for collecting the log data. When this was finished, the drill string had become stuck and we were unable to raise it. We spent the next 2.75 h trying to free the drill string (installed the top drive, pumped, and applied overpull). Finally, at 2115 h on 5 April, we were able to resume raising the bit up the hole with the top drive.

We deployed the subsea camera system as we finished pulling the drill string out of Hole U1500B; the bit cleared the seafloor at 0430 h on 6 April. We offset the ship 20 m to the west, released the bit on the seafloor at 0600 h, reentered Hole U1500B at 0840 h, and set the end of the pipe at a logging depth of 35.4 m (inside casing). After the camera system was recovered at 1100 h on 6 April, we prepared the rig floor for logging. We assembled a modified triple combo tool string that contained the following tools:

- Dipole Sonic Imager Tool (DSI) for acoustic velocity,
- High-Resolution Laterolog Array (HRLA)/Phasor Dual Induction-Spherically Focused Resistivity Tool (DIT) for electrical resistivity,
- Hostile Environment Litho-Density Sonde (HLDS) without the source for caliper data, and
- Hostile Environment Natural Gamma Ray Sonde (HNGS)/Enhanced Digital Telemetry Cartridge (EDTC-B) for NGR.

At 1345 h on 6 April, we started lowering to the seafloor. The tool passed through the base of the casing at 842 m and into the open hole. It was unable to pass an obstruction at 1133 m, and log data were collected from there up to the base of the casing. The modified triple combo tool string arrived back on the rig floor at 2145 h on 6 April.

We assembled an FMS tool string consisting of the FMS to collect borehole resistivity images and the HNGS and EDTC-B to collect NGR data and for correlating with the previous logging runs. This second tool string was only able to reach 1044 m, 89 m shallower than the first logging string. We opened the FMS arms and collected data from that depth up to the bottom of the casing at 842 m. Our last operation for Expedition 367 was to conduct a check shot experiment with the VSI (geophone). We started assembling the VSI tool string at 0700 on 7 April. It consisted of the VSI sonde and ETDC-B. Routine IODP protected-species procedures were implemented leading up to and throughout use of the seismic source. The VSI tool string reached a total depth of 1031 m, and data were collected at that depth as well as at one station in the bottom of the casing at 783 m. The VSI tool string arrived back on the rig floor at 1430 h on 7 April. After the rig floor was cleared of logging equipment at 1530 h on 7 April, we pulled the end of the pipe out of the hole (1523 h on 7 April) and recovered the drill string. We conducted operations at Site U1500 for a total of 30.3 days (5.5 days in Hole U1500A; 24.8 days in Hole U1500B).

At 0100 h on 8 April, we started our transit to Hong Kong. Expedition 367 ended with the first line ashore at 0800 h on 9 April.

## Education and outreach

Expedition 367 had a team of two Onboard Outreach Officers: one teacher from Italy and one journalist from China. The Officers communicated the goals of their jobs on the ship to all scientists at the very beginning of the expedition. This presentation gave examples of how the Onboard Outreach team could be a resource for the scientists to share their research during the expedition to the general public. The two Onboard Outreach Officers had different ap-

proaches and targets in their responsibilities; this report includes both.

The Officer/Teacher worked with three different outreach tools: webcasts, social media, and educational activities.

## Webcasts

The Onboard Outreach Officer interacted with locations on shore to share the scientific goals and progress of the expedition by using iPads and the videoconferencing software, Zoom. The video connection schedule was prepared using a public Google calendar, direct contact with teachers to advertise the opportunity, and requests from scientists onboard the *JOIDES Resolution*. Each webcast was led by a scientist who spoke the native language of the shore-based school (primarily Italian and English). The connections were used to reach students from primary schools to universities (both graduate and undergraduate levels) and professional development workshops. A typical session was approximately 1 h and was divided into the following parts:

- Identification of the geographical location and presentation of the geological questions addressed by the expedition,
- Tour of the ship with a close look at the derrick, the rig floor, and the catwalk,
- Tour of the labs with questions to the scientists present (usually sedimentologists, core describers, paleomagnetists, and paleontologists), and
- Opportunities for the students to ask questions.

A total of 99 events reached ~7100 students in 7 different countries (Italy, China, USA, France, Germany, Spain, and Argentina)

Before every video connection, the Onboard Outreach Officer interacted with the schools by sending the teachers some selected educational material about the *JOIDES Resolution*, the seafloor drilling research, and the scientific topics related to Expedition 367 (e.g., tectonic plates). After the video connection, a postsurvey was sent to all the teachers and participants (from Europe and America).

## Social media

The Onboard Outreach Officer maintained four social media accounts during the expedition: the *JOIDES Resolution's* Facebook page, Twitter feed, and Instagram account, and a blog at **http://joidesresolution.org**. The total number of posts on the blog was 40. The blog posts were divided into different areas: science on board, behind the science, life on a ship, and education and outreach. Each post required some time to collect information (through interviews, for example) and was reviewed for accuracy before publishing. The total number of Facebook posts was 40. The posts were viewed ~95,000 times and replied to, liked, or shared ~7000 times. A total of ~40 posts was published on Twitter and Instagram, too.

The Onboard Outreach Officer also hosted a Reddit Science "Ask Me Anything" session, answering 24 questions from the public over the course of 2 h. Three members of the science party (basically all the English native speakers on shift at the time of the session) assisted with this session, which is permanently archived at **https://www.reddit.com/r/science/comments/618g7f/science_ama_series_we_are_scientists_on_board_the/**.

Midway through the expedition, the Onboard Outreach Officer held a contest for schools to guess the depth of the basement at Site U1500. One third of the schools that connected to the ship via webcasts participated in the contest.

## Media

The Onboard Outreach Officer facilitated interviews between reporters from national media outlets and the science party. She provided background information, photographs, and video footage. This resulted in:

- One interview with an Italian journalist for an online article: **https://oggiscienza.it/2017/03/08/joides-perforazione-oceanica-geologia/**;
- One interview with an Italian journalist that resulted in an online video interview and an article in the scientific rubric of the newspaper: **http://www.repubblica.it/scienze/2017/03/19/foto/ricercatori_internazionali_sulla_nave_education_and_outreach_officer-160942447/1/#1**;
- One radio interview: **http://www.radio3.rai.it/dl/portaleRadio/media/ContentItem-94c91c08-f402-4a11-9406-161452bb3513.html**; and
- One outreach event with a German television station: **https://hannover.sat1regional.de/aktuell/article/unterirdisch-wissenschaftsshow-fuer-rund-750-schueler-in-braunschweig-228928.html**.

## Educational material

The Onboard Outreach Officer recorded several interviews with scientists and technical staff. These recorded interviews resulted in videos discussing the research activities onboard. These were also edited in different languages. Other videos, interviews and pictures collected during the expedition will be used for post-expedition activities to develop additional educational materials.

## Chinese media outreach

During the 2 months of Expedition 367, the Xinhua News Agency had broadcasts with >30 news articles, including 180 photos. These reports described the history and achievements of IODP, the research progress of ocean drilling in the SCS, and the important progress of Expedition 367. These reports included overviews of each scientist's research. These reports with pictures and texts were widely reproduced in the Chinese media and the network, which attracted a lot of attention for IODP drilling and scientific research in the SCS.

# References

Barckhausen, U., and Roeser, H.A., 2004. Seafloor spreading anomalies in the South China Sea revisited. *In* Clift, P., Wang, P., Kuhnt, W., and Hayes, D. (Eds.), *Continent-Ocean Interactions within East Asian Marginal Seas.* Geophysical Monograph, 149:121–125. **http://dx.doi.org/10.1029/149GM07**

Briais, A., Patriat, P., and Tapponnier, P., 1993. Updated interpretation of magnetic anomalies and seafloor spreading stages in the South China Sea: implications for the Tertiary tectonics of Southeast Asia. *Journal of Geophysical Research: Solid Earth,* 98(B4):6299–6328. **http://dx.doi.org/10.1029/92JB02280**

Brune, S., Heine, C., Clift P.D., and Pérez-Gussinyé, M., 2017. Rifted margin architecture and crustal rheology: reviewing Iberia-Newfoundland, Central South Atlantic, and South China Sea. *Marine and Petroleum Geology,* 79:257–281. **https://doi.org/10.1016/j.marpetgeo.2016.10.018**

Dick, H.J.B., Lin, J., and Schouten, H., 2003. An ultraslow-spreading class of ocean ridge. *Nature,* 426(6965):405–412. **http://dx.doi.org/10.1038/nature02128**

Doré, T., and Lundin, E., 2015. Research focus: hyperextended continental margins—knowns and unknowns. *Geology,* 43(1):95–96. **https://doi.org/10.1130/focus012015.1**

Franke, D., Savva, D., Pubellier, M., Steuer, S., Mouly, B., Auxietre J.-L., Meresse, F., and Chamot-Rooke, N., 2013. The final rifting evolution in the South China Sea. *Marine and Petroleum Geology,* 58(Part B):704–720. **http://dx.doi.org/10.1016/j.marpetgeo.2013.11.020**

Hall, R., 2002. Cenozoic geological and plate tectonic evolution of SE Asia and the SW Pacific: computer-based reconstructions, model and animations. *Journal of Asian Earth Sciences,* 20(4):353–431. **http://dx.doi.org/10.1016/S1367-9120(01)00069-4**

Huismans, R., and Beaumont, C., 2011. Depth-dependent extension, two-stage breakup and cratonic underplating at rifted margins. *Nature,* 473(7345):74–78. **http://dx.doi.org/10.1038/nature09988**

Huismans, R.S., and Beaumont, C., 2008. Complex rifted continental margins explained by dynamical models of depth-dependent lithospheric extension. *Geology,* 36(2):163–166. **http://dx.doi.org/10.1130/G24231A.1**

Lester, R., McIntosh, K., Van Avendonk, H.J.A., Lavier, L., Liu, C.-S., and Wang, T.K., 2013. Crustal accretion in the Manila trench accretionary wedge at the transition from subduction to mountain-building in Taiwan. *Earth and Planetary Science Letters,* 375:430–440. **http://dx.doi.org/10.1016/j.epsl.2013.06.007**

Li, C.-F., Lin, J., and Kulhanek, D.K., 2013. *Expedition 349 Scientific Prospectus: South China Sea Tectonics.* International Ocean Discovery Program. **http://dx.doi.org/10.2204/iodp.sp.349.2013**

Li, C.-F., Lin, J., Kulhanek, D.K., Williams, T., Bao, R., Briais, A., Brown, E.A., Chen, Y., Clift, P.D., Colwell, F.S., Dadd, K.A., Ding, W., Hernández-Almeida, I., Huang, X.-L., Hyun, S., Jiang, T., Koppers, A.A.P., Li, Q., Liu, C., Liu, Q., Liu, Z., Nagai, R.H., Peleo-Alampay, A., Su, X., Sun, Z., Tejada, M.L.G., Trinh, H.S., Yeh, Y.-C., Zhang, C., Zhang, F., Zhang, G.-L., and Zhao, X., 2015a. Expedition 349 summary. *In* Li, C.-F., Lin, J., Kulhanek, D.K., and the Expedition 349 Scientists, *South China Sea Tectonics.* Proceedings of the International Ocean Discovery Program, 349: College Station, TX (International Ocean Discovery Program). **http://dx.doi.org/10.14379/iodp.proc.349.101.2015**

Li, C.-F., Lin, J., Kulhanek, D.K., Williams, T., Bao, R., Briais, A., Brown, E.A., Chen, Y., Clift, P.D., Colwell, F.S., Dadd, K.A., Ding, W., Hernández-Almeida, I., Huang, X.-L., Hyun, S., Jiang, T., Koppers, A.A.P., Li, Q., Liu, C., Liu, Q., Liu, Z., Nagai, R.H., Peleo-Alampay, A., Su, X., Sun, Z., Tejada, M.L.G., Trinh, H.S., Yeh, Y.-C., Zhang, C., Zhang, F., Zhang, G.-L., and Zhao, X., 2015b. Site U1435. *In* Li, C.-F., Lin, J., Kulhanek, D.K., and the Expedition 349 Scientists, *South China Sea Tectonics.* Proceedings of the International Ocean Discovery Program, 349: College Station, TX (International Ocean Discovery Program). **http://dx.doi.org/10.14379/iodp.proc.349.107.2015**

Li, C.-F., Wang, P., Franke, D., Lin, J., and Tian, J., 2012a. Unlocking the opening processes of the South China Sea. *Scientific Drilling,* 14:55–59. **http://dx.doi.org/10.2204/iodp.sd.14.07.2012**

Li, C.-F., Xu, X., Lin J., Sun, Z., Zhu, J., Yao, Y., Zhao, X., Liu, Q., Kulhanek, D.K., Wang, J., Song, T., Zhao, J., Qiu, N., Guan, Y., Zhou, Z, Williams, T., Bao, R., Briais, A., Brown, E.A., Chen, Y., Clift, P.D., Colwell, F.S., Dadd, K.A., Ding, W., Hernández Almeida, I., Huang, X.-L., Hyun, S., Jiang, T., Koppers, A.A.P., Li, Q., Liu, C., Liu, Z., Nagai, R.H., Peleo-Alampay, A., Su, X., Tejada, M.L.G., Trinh, H.S., Yeh, Y.-C., Zhang, C., Zhang, F., and Zhang, G.-L., 2014. Ages and magnetic structures of the South China Sea constrained by deep tow magnetic surveys and IODP Expedition 349. *Geochemistry, Geophysics, Geosystems,* 15(12):4958–4983. **http://dx.doi.org/10.1002/2014GC005567**

Li, J., Ding, W., Wu, Z., Zhang, J., and Dong, C., 2012b. The propagation of seafloor spreading in the southwestern subbasin, South China Sea. *Chinese Science Bulletin,* 57(24):3182–3191. **http://dx.doi.org/10.1007/s11434-012-5329-2**

McIntosh, K., Lavier, L., van Avendonk, H., Lester, R., Eakin, D., and Liu, C.-S., 2014. Crustal structure and inferred rifting processes in the northeast South China Sea. *Marine and Petroleum Geology,* 58(Part B):612–626. **http://dx.doi.org/10.1016/j.marpetgeo.2014.03.012**

McIntosh, K., van Avendonk, H., Lavier, L., Lester, W.R., Eakin, D., Wu, F., Liu, C.-S., and Lee, C.-S., 2013. Inversion of a hyper-extended rifted margin in the southern Central Range of Taiwan. *Geology,* 41(8):871–874. **http://dx.doi.org/10.1130/G34402.1**

Pérez-Gussinyé, M., Phipps Morgan, J., Reston, T.J., and Ranero, C.R., 2006. The rift to drift transition at non-volcanic margins: insights from numerical modelling. *Earth and Planetary Science Letters,* 244(1–2):458–473. **http://dx.doi.org/10.1016/j.epsl.2006.01.059**

Pérez-Gussinyé, M., and Reston, T.J., 2001. Rheological evolution during extension at nonvolcanic rifted margins: onset of serpentinization and development of detachments leading to continental breakup. *Journal of Geophysical Research: Solid Earth,* 106(B3):3961–3975. **http://dx.doi.org/10.1029/2000JB900325**

Reston, T.J., 2009. The structure, evolution and symmetry of the magma-poor rifted margins of the North and Central Atlantic: a synthesis. *Tectonophysics,* 468(1–4):6–27. **http://dx.doi.org/10.1016/j.tecto.2008.09.002**

Shi, H., and Li, C.-F., 2012. Mesozoic and early Cenozoic tectonic convergence-to-rifting transition prior to opening of the South China Sea. *International Geology Review,* 54(15):1801–1828. **http://dx.doi.org/10.1080/00206814.2012.677136**

Sibuet, J.-C., and Tucholke, B.E., 2012. The geodynamic province of transitional lithosphere adjacent to magma-poor continental margins. *Geological Society Special Publication,* 369:429–452. **http://dx.doi.org/10.1144/SP369.15**

Sun, Z., Liu, S., Pang, X., Jiang, J., and Mao, S., 2016a. Recent research progress on the rifting-breakup process in passive continental margins. *Journal of Tropical Oceanography,* 35(1):1–16. (in Chinese with English abstract) **http://dx.doi.org/10.11978/2015030**

Sun, Z., Stock, J., Jian, Z., McIntosh, K., Alvarez-Zarikian, C.A., and Klaus, A., 2016b. *Expedition 367/368 Scientific Prospectus: South China Sea Rifted Margin.* International Ocean Discovery Program. **http://dx.doi.org/10.14379/iodp.sp.367368.2016**

Sun, Z., Xu, Z., Sun, L., Pang, X., Yan, C., Li, Y., Zhao, Z., Wang, Z., and Zhang, C., 2014. The mechanism of post-rift fault activities in Baiyun sag, Pearl River Mouth Basin. *Journal of Asian Earth Sciences,* 89:76–87. **https://doi.org/10.1016/j.jseaes.2014.02.018**

Sutra, E., and Manatschal, G., 2012. How does the continental crust thin in a hyperextended rifted margin? Insights from the Iberia margin. *Geology,* 40(2):139–142. **http://dx.doi.org/10.1130/G32786.1**

Wang, P., Prell, W.L., Blum, P., et al., 2000. *Proceedings of the Ocean Drilling Program, Initial Reports,* 184: College Station, TX (Ocean Drilling Program). **http://dx.doi.org/10.2973/odp.proc.ir.184.2000**

Wang, T.K., Chen, M.-K., Lee, C.-S., and Xia, K., 2006. Seismic imaging of the transitional crust across the northeastern margin of the South China Sea. *Tectonophysics,* 412(3–4):237–245. **http://dx.doi.org/10.1016/j.tecto.2005.10.039**

Wei, X.-D., Ruan, A.-G., Zhao, M.-H., Qiu, X.-L., Li, J.-B., Zhu, J.-J., Wu, Z.-L., and Ding, W.-W., 2011. A wide-angle OBS profile across the Dongsha uplift and Chaoshan depression in the mid-northern South China Sea. *Chinese Journal of Geophysics,* 54(6):1149–1160. **http://dx.doi.org/10.1002/cjg2.1691**

Whitmarsh, R.B., Manatschal, G., and Minshull, T.A., 2001. Evolution of magma-poor continental margins from rifting to seafloor spreading. *Nature,* 413(6852):150–154. **http://dx.doi.org/10.1038/35093085**

Yan, P., Zhou, D., and Liu, Z., 2001. A crustal structure profile across the northern continental margin of the South China Sea. *Tectonophysics,* 338(1):1–21. **http://dx.doi.org/10.1016/S0040-1951(01)00062-2**

Zhou, D., Sun, Z., Chen, H., Xu, H., Wang, W., Pang, X., Cai, D., and Hu, D., 2008. Mesozoic paleogeography and tectonic evolution of South China Sea and adjacent areas in the context of Tethyan and Paleo-Pacific interconnections. *Island Arc,* 17(2):186–207. **http://dx.doi.org/10.1111/j.1440-1738.2008.00611.x**

Zhou, X.M., and Li, W.X., 2000. Origin of late Mesozoic igneous rocks in southeastern China: implications for lithosphere subduction and underplating of mafic magmas. *Tectonophysics,* 326(3–4):269–287. **http://dx.doi.org/10.1016/S0040-1951(00)00120-7**

Table T1. Expedition 367 hole summary. — = no data.

| Hole | Proposed site | Location | Water depth (m) | Total penetration (m) | Cored interval (m) | Drilled interval without coring (m) | Core recovery (m) | Core recovery (%) | Time in hole (days) | Cores (N) | Depth of 10.75 inch casing (m) |
|---|---|---|---|---|---|---|---|---|---|---|---|
| U1499A | SCSII-14A | 18° 24.5698′N 115° 51.5881′E | 3760.2 | 659.2 | 659.2 | 0.0 | 417.05 | 63 | 7.2 | 71 | — |
| U1499B | | 18° 24.5705′N 115° 51.5990′E | 3758.1 | 1081.8 | 426.8 | 655.0 | 150.64 | 35 | 14.9 | 44 | 651 |
| | | Site U1499 totals: | | 1741.0 | 1086.0 | 655.0 | 567.69 | 52 | 22.1 | 115 | — |
| U1500A | SCSII-8B | 18° 18.2762′N 116° 13.1916′E | 3801.7 | 854.6 | 329.8 | 524.8 | 93.55 | 28 | 5.5 | 34 | — |
| U1500B | | 18° 18.2707′N 116° 13.1951′E | 3801.7 | 1529.0 | 683.0 | 846.0 | 278.80 | 41 | 24.8 | 81 | 842 |
| | | Site U1500 totals: | | 2383.6 | 1012.8 | 1370.8 | 372.35 | 37 | 30.3 | 115 | — |
| | | Expedition 367 totals: | | 4124.6 | 2098.8 | 2025.8 | 940.04 | 45 | 52.4 | 230 | 1493 |

Figure F1. Seismic data coverage and magnetic anomalies of the South China Sea Basin, Expedition 367. Black lines = ocean-bottom seismometer refraction data. Other seismic lines are mostly multichannel seismic reflection data. White stars = Expedition 367 and 368 drill sites. ODP Leg 184 (red squares) and IODP Expedition 349 (red circles) sites are shown with site numbers. For more details, see Figure **F4**.
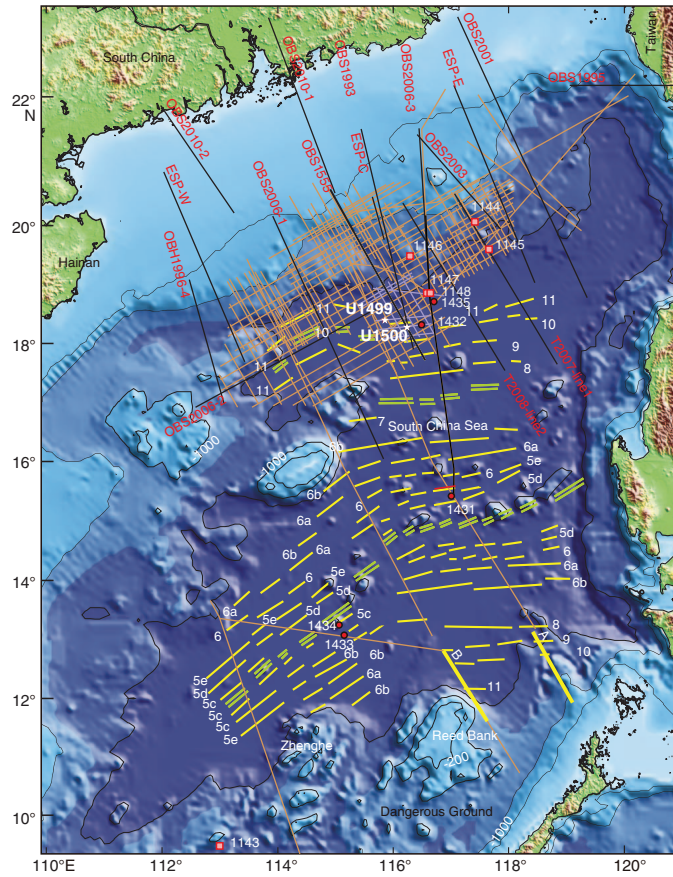
Figure F2. A–D. Schematic development of continental breakup initiated by a simple shear along a deep, low-angle fault. B–D are slightly modified from Huismans and Beaumont (2011) and illustrate modeling-based stages of extension at magma-poor rifted margins of the Iberia-Newfoundland type. Key features of D are thinning of the upper crust, juxtaposition of lower crust (e.g., Site U1499), and serpentinized mantle (Site U1500) between the outer margin and igneous oceanic crust. UP = upper plate, LP = lower plate.
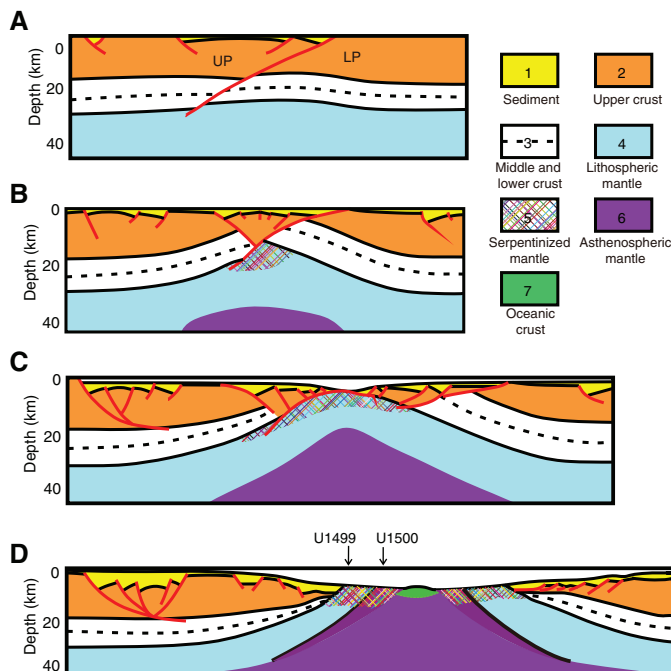
Figure F3. Northern South China Sea margin with seismic coverage of 2-D, time-migrated multichannel seismic reflection seismic data and ocean-bottom seismometer data. Key seismic lines used for planning of the drilling transect are marked in thick blue lines. White stars = Expedition 367 drill sites. Red lines = magnetic lineations within the ocean crust. Magnetic chron number is after Briais et al. (1993).
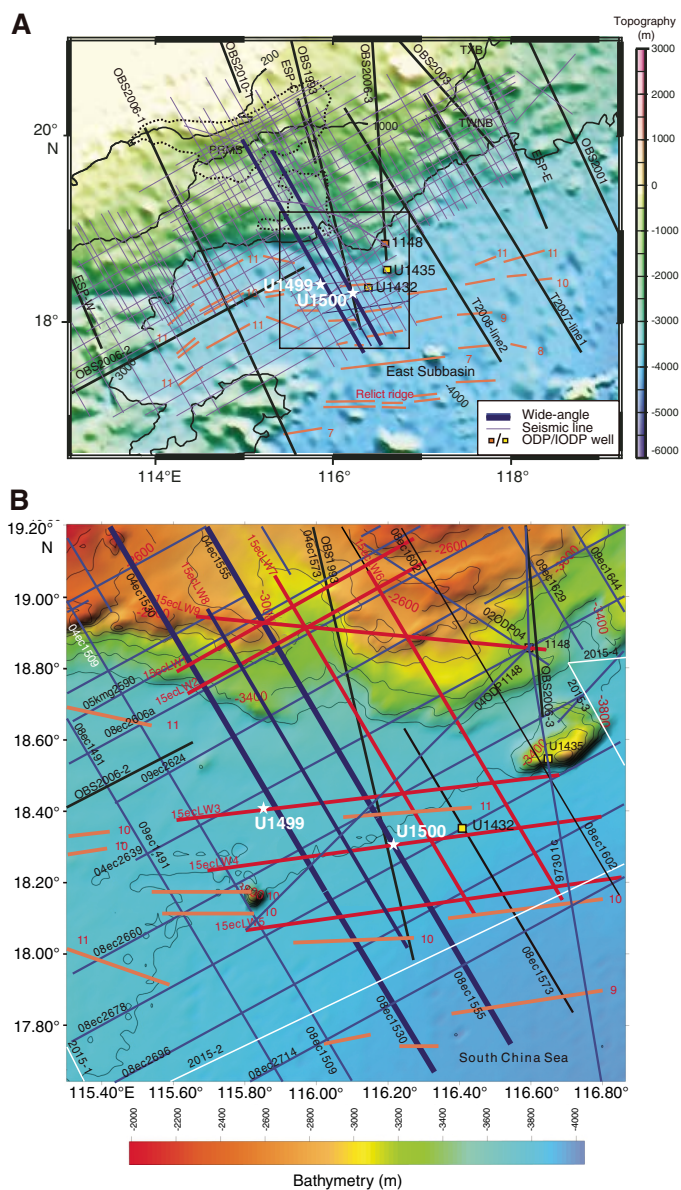
Figure F4. Two-way traveltime to (A) basement (Tg unconformity) and (B) Reflector T60. The proposed drilling transect (thick black line) is located approximately at the center of a margin segment bounded to the southwest by a transform fault. The northeastern boundary of the margin segment is located around Expedition 349 Site U1435. In this location, the outer margin high and Ridge A seem to coalesce, and Ridges B and C of the continent–ocean transition become indistinct toward the northeast within the next margin segment. Note that the outer margin high is slightly oblique to more parallel Ridges A, B, and C.
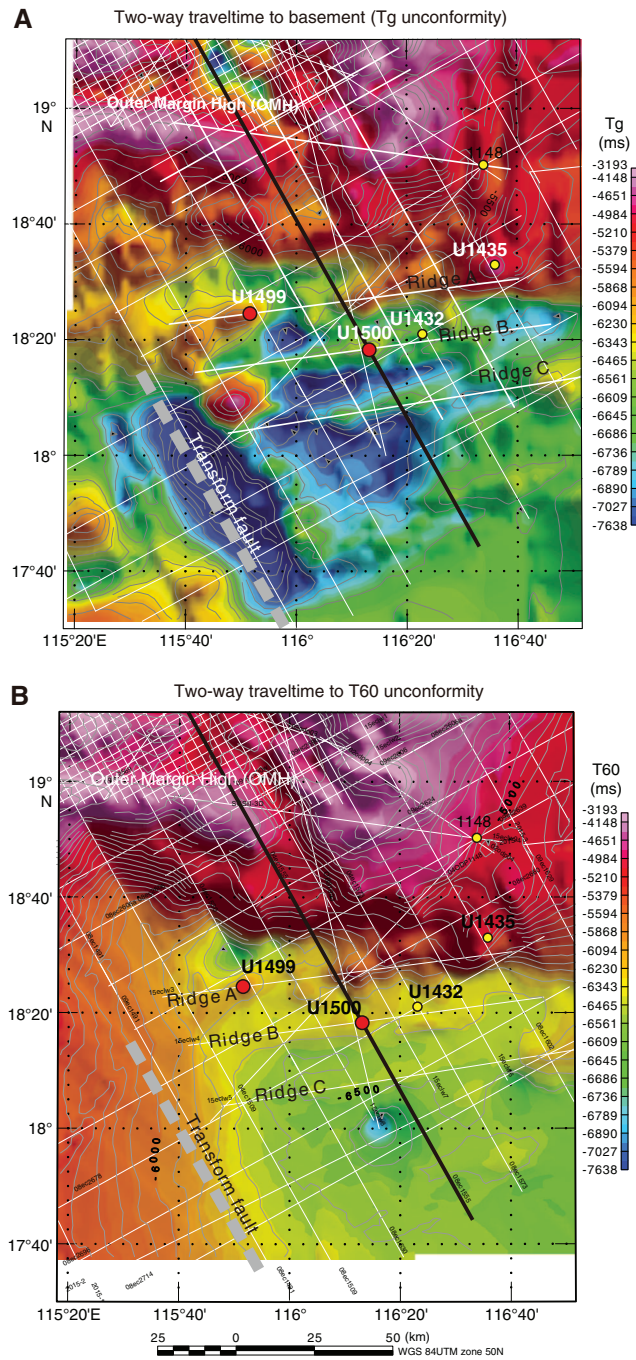
Figure F5. Deep crustal time-migrated seismic reflection data (A) without interpretation and (B) with interpretation. Note the rather thin lower crust (two layers) above a strong Mohorovicic seismic discontinuity (Moho) reflector that can be followed oceanward. Moho reflection is weak to absent seaward from around the interpreted continent–ocean boundary (COT). Wide-angle seismic data (Yan et al., 2001) confirm ~6 km thick ocean crust (OC) to be present seaward of the COT. A large detachment fault ~150 km inland of the COT separates more stable crust landward from that of highly extended crust seaward. An outer margin high (OMH) is a fairly consistent feature margin along this margin segment. Key seismic unconformities are shown in purple (T70; ~32 Ma breakup unconformity?) and blue (T60; ~23 Ma regional basin event). These ages are inferred from long-distance (>100 km) correlation of seismic unconformities with industry holes and ODP Leg 184 Site 1148 (T60). These ages need confirmation by coring, and are only tentative. Tg unconformity (green) is basement. Approximate position of seafloor magnetic anomalies with chron numbers are shown by arrows. Seismic data is from Line 04ec1555-08ec1555 (courtesy of the Chinese National Offshore Oil Corporation [CNOOC]). Location of line is shown in Figure F3. CDP = common depth point; C11?, C10?, and C9? = possible Chrons. MSB = midslope basin.
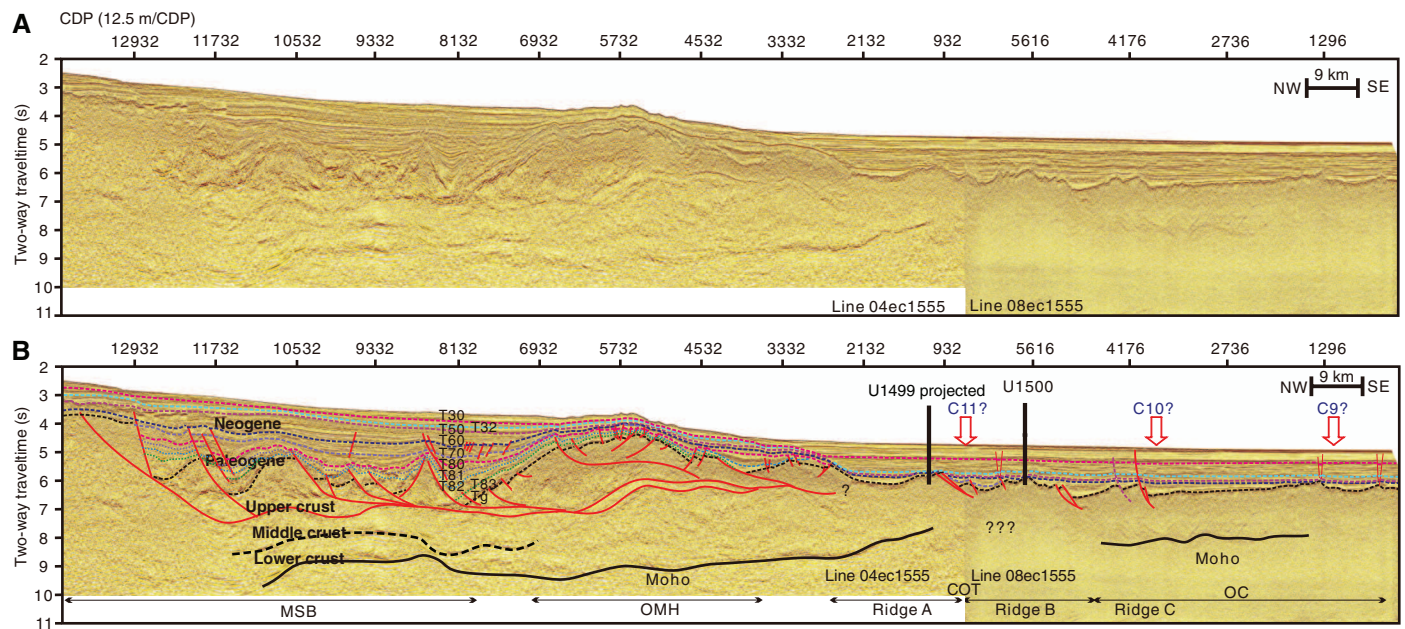
Figure F6. Planned and implemented Expedition 367 operations. APC = advanced piston corer, XCB = extended core barrel, RCB = rotary core barrel

Figure F7. Lithostratigraphic summary of Site U1499 stratigraphy.



### Site U1499 lithostratigraphy unit description

Unit I (0–48.85 m)
Dark greenish gray bioclast-rich clay, with thin clayey silt and
sand interbeds.

Unit II (48.85–100.04 m)
Greenish gray clay-rich calcareous ooze and dark greenish gray
nannofossil-rich clay.

Unit IIIA (100.04–181.80 m)
Dark greenish gray clay, with very thin (<1 cm) clayey silt interbeds.

Unit IIIB (181.80–333.65 m)
Dark greenish gray clay, with thin (2–5 cm) clayey silt and
nannofossil/foraminifer interbeds.

Unit IV (333.65–404.90 m)
Dark greenish gray silty sand, with clay interbeds.

Unit V (404.90–469.45 m)
Dark greenish gray clay, with thin (<5 cm) clayey silt and
foraminifer sand interbeds. Clay sediments are heavily bioturbated.

Unit VI (469.45–618.30 m)
Dark greenish gray silty sand, with clay interbeds.

Unit VII (618.30–761.70 m)
Dark greenish to dark gray sandstone and claystone, with siltstone
interbeds. Sections with very low recovery are assumed to be
primarily composed of nonlithified sand.

Unit VIIIA (761.70–892.10 m)
Dark brownish claystone, with greenish to gray siltstone, calcareous-rich
claystone with silt, and foraminifer sandstone interbeds.

Unit VIIIB (892.10–929.02 m)
Reddish brown to reddish gray clay-rich nannofossil chalk and
clay-rich chalk.

Unit IXA (929.04–933.28 m)
Brownish to greenish sandstone with polymict clasts, sandstone
with angular pebbles, and matrix-supported breccia.

Unit IXB (933.28–933.35 m)
Dark gray matrix-supported breccia with polymict clasts.

Unit IXC (933.35–1081.80 m)
Gray to dark gray gravel, with silty sand intervals.
The cores are completely fragmented and
recovered as pebbles and cobbles.

Legend:
- Clay/Claystone
- Silt/Siltstone
- Sand/Sandstone
- Gravel
- Breccia
- Carbonate

Figure F8. Lithostratigraphic summary of Site U1500 stratigraphy.



Site U1500 lithostratigraphy unit description

**Unit I (378.20–410.00 m)**
Dark greenish gray clay with silt interbeds and greenish gray clay with nannofossils.

**Unit II (410.00–494.60 m)**
Dark greenish gray sandstone and siltstone, with claystone interbeds.

Drilled Interval 14 (494.60–641.20 m) was washed down without coring.

**Unit III (641.20–892.44 m)**
Dark greenish gray to dark gray sandstone and claystone, with thin siltstone interbeds. Mudclasts occur in sandstone layers.

**Unit IV (892.44–1233.30 m)**
Dark greenish gray to dark gray sandstone with claystone and siltstone interbeds. Very low recovery (15%).

**Unit VA (1233.30–1272.10 m)**
Dark reddish brown claystone.

**Unit VB (1272.10–1310.98 m)**
Dark reddish brown calcareous-rich claystone and clay-rich chalk.

**Unit VI (1310.98–1370.33 m)**
Dark greenish gray silty claystone with biogenic carbonate and dark gray sandstone.

**Unit VII (1370.33–1379.10 m)**
Very dusky red and greenish gray claystone.

**Unit VIII (1379.10–1529.00 m)**
Basalt with occasional brownish claystone inclusions.

Clay/Claystone
Silt/Siltstone
Sand/Sandstone
Ooze/Chalk
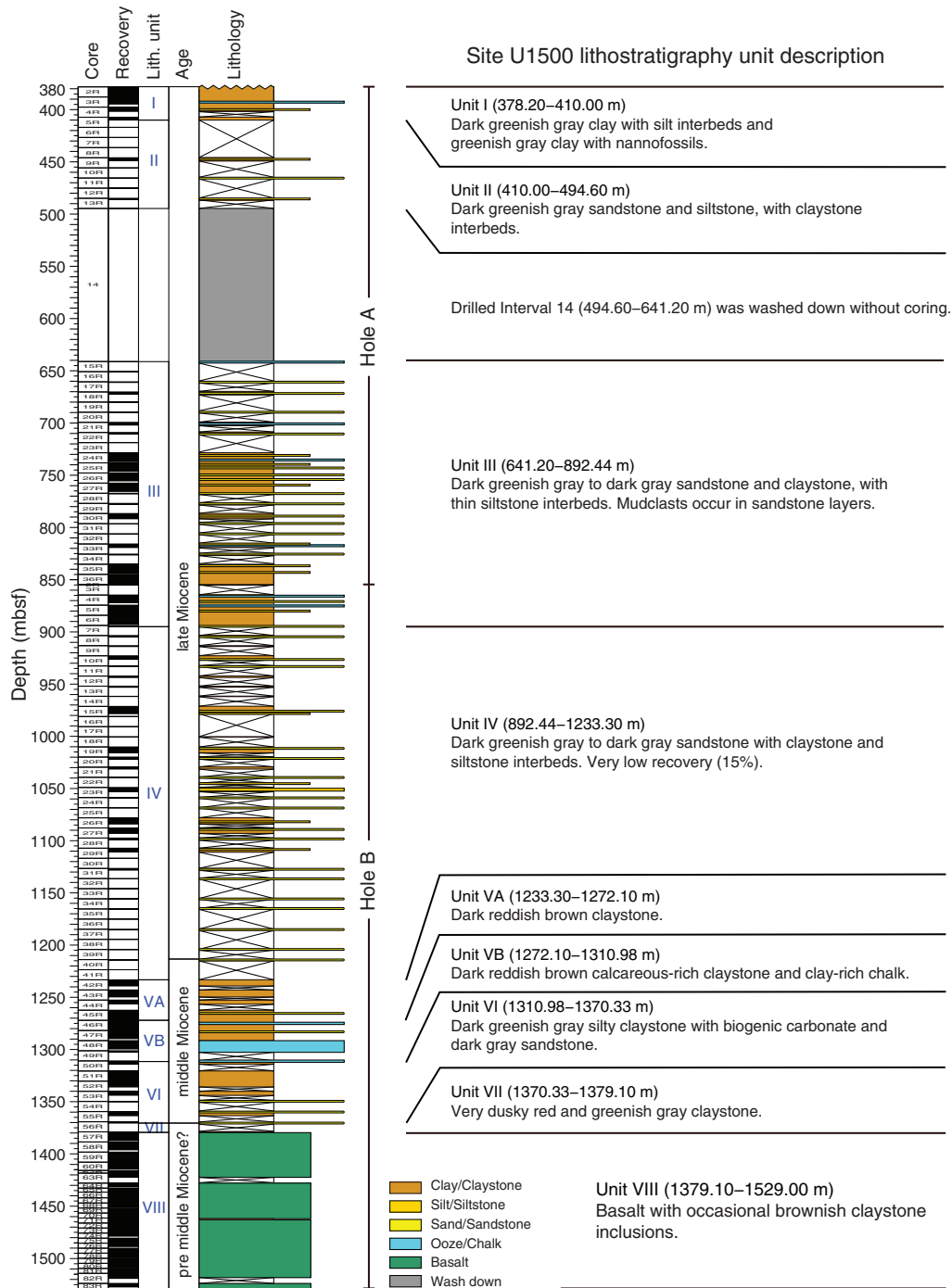Basalt
Wash down

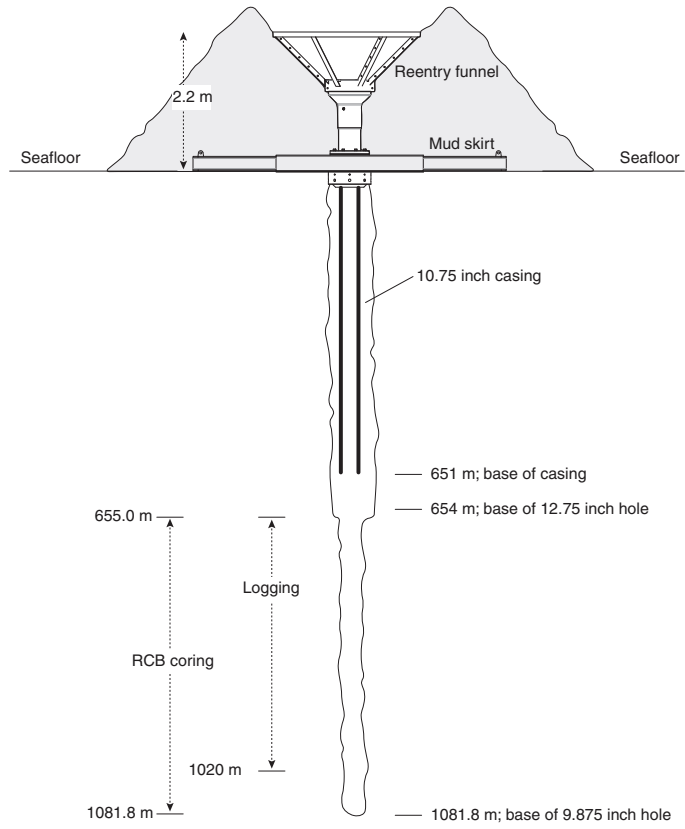Figure F9. Hole U1499B reentry system and casing. RCB = rotary core barrel.

Figure F10. Hole U1500B reentry system and casing. RCB = rotary core barrel.